International Journal of Secondary Metabolite
2022, Vol. 9, No. 4, 467–492
https://doi.org/10.21448/ijsm.1107685
Published at https://dergipark.org.tr/en/pub/ijsm
Research Article

Pharmacokinetics, drug-likeness, antibacterial and antioxidant activity of secondary metabolites from the roots extracts of *Crinum abyssinicum* and *Calotropis procera* and *in silico* molecular docking study

Getachew Tegegn[1], Yadessa Melaku[1], Rajalakshmanan Eswaramoorthy[2], Milkyas Endale[1,*]

[1]Department of Applied Chemistry, School of Applied Natural Science, Adama Science and Technology University, P.O. Box 1888, Adama, Ethiopia
[2]Department of Biomaterials, Saveetha Dental College and Hospitals, Saveetha Institute of Medical and Technical Sciences, Saveetha University, Chennai-600 077, India.

Abstract: *Crinum abyssinicum* and *Calotropis procera* were traditionally used for the treatment of different diseases such as hypertension, diabetes, hepatitis B, skin infection, anticancer, asthma, fever, and diarrhea. The structures of the compounds were characterized by ^{1}H NMR, ^{13}C NMR, and DEPT-135 spectra. Compounds **1-3** were reported herein for the first time from the species of *C. abyssinicum*. The DCM/MeOH (1:1) and MeOH roots extracts of *C. abyssinicum* showed significant inhibitory activity against *S. aureus* and *P. aeruginosa* with a mean inhibition zone of 16.67 ± 1.20 and 16.33 ± 0.33 mm, respectively. Compounds **4** and **5** showed promising activity against *E. coli* with a mean inhibition zone of 17.7 ± 0.8 and 17.7 ± 1.2 mm, respectively. The results of DPPH activity showed the DCM: MeOH (1:1) and MeOH roots extracts of *C. abyssinicum* inhibited the DPPH radical by 52.86 ± 0.24 % and 45.6 ± 0.11 %, respectively, whereas compound **5** displayed 85.7 % of inhibition. The drug-likeness analysis showed that compounds **2-4** satisfy Lipinski's rule of five with zero violations. Compounds **2**, and **6** showed binding affinities of −6.0, and −6.7 kcal/mol against *E. coli* DNA gyrase B, respectively, while **3** and **5** showed −5.0 and −5.0 kcal/mol, respectively against human peroxiredoxin 5. Therefore, the *in vitro* antibacterial, radical scavenging activity along with the molecular docking analysis suggest the potential use of the extracts of *C. abyssinicum* and compounds **2, 5, 6,** and **3, 5** can be considered as promising antibacterial agents and free radical scavengers, respectively.

ARTICLE HISTORY
Received: Apr. 23, 2022
Revised: Oct. 11, 2022
Accepted: Nov. 30, 2022

KEYWORDS
Crinum abyssinicum,
Calotropis procera,
Antibacterial,
Antioxidant
ADMET,
Molecular docking.

1. INTRODUCTION

The genus *Crinum* is one of the medicinal plants that belong to the family Amaryllidaceae. Globally, around 180 Crinum species were described and widely distributed in Africa, America, southern Asia, and Australia (Lawal & Dangoggo, 2014). Out of these, four species are found in Ethiopia *i.e.*, *Crinum abyssinicum, Crinum bambusetum, Crinum macowanii*, and *Crinum ornatum* (Nordal & Sebsebe, 2010). *Crinum abyssinicum* and *Crinum bambusetum* are endemic species of Ethiopia (Nordal & Sebsebe, 2010). *Crinum abyssinicum* is a species of bulbous

*CONTACT: Milkyas Endale ✉ milkyasendale@yahoo.com Department of Applied Chemistry, School of Applied Natural Science, Adama Science and Technology University, P.O. Box 1888, Adama, Ethiopia

ISSN-e: 2148-6905 / **© IJSM 2022**

plant that belongs to the family of the Amaryllidaceae (Figure 1). In Ethiopia, it is commonly known as shinkurta/bokolo Werabessa/ Murquffaa/ Chopi in Afan Oromo, Yejib Shinkurt in Amharic, Galadiweese in Sidamigna (Abebe *et al*., 2003). In Ethiopia, *Crinum* species have been reported to be used in various health care systems for the treatment of a variety of diseases such as hypertension and diabetes (Regassa, 2013), animals' internal parasites (Tamiru *et al*., 2013), skin infection (Yineger *et al*., 2008), rheumatoid arthritis (Kloos *et al*., 2014), snake bite (Mekuanent *et al*., 2016), malaria (Asnakech *et al*., 2019) and antitumor (Teklehaymanot & Giday, 2007). Traditionally the dried roots of *C. abyssinicum* mixed with water or butter is applied topically or oral.

Figure 1. (a) Aerial part and (b) bulb of *C. abyssinicum* (Illubabor, Oromia, Picture taken by Melaku Tegegn on November 20, 2021).

(a)

(b)

Crinum species have been subjected to extensive chemical and biological investigations due to their richness in pharmacologically active principles (Wildman, 1960). A large number of alkaloids and non-alkaloid compounds have been reported from different *Crinum* species (Refaat *et al*., 2012; 2013). Amaryllidaceae alkaloids, augustamine (Ali *et al*., 1983; Ramadan, 1986; Machocho *et al*., 2004), *β*-carboline, phenanthridine (Razafimbelo *et al*., 1996), sceletium (Döpke *et al*., 1981), ismine (Ghosal, 1981; Highet & Ismine, 1961) and clivimine type alkaloids were reported from the genus. Other secondary metabolites including flavonoids, chromones, coumarins, terpenoids, steroids, phenolics, simple glycosides, and long-chain hydrocarbons were also reported (Refaat *et al*., 2013). In Ethiopia, the bulb extract, 6-hydroxycrinamine, and lycorine possessed significant antiproliferative activity, lycorine being the most active exhibiting GI_{50} values of 2.8 μg/mL and 3.4 μg/mL against A2780 and MV4-11 cells, respectively (Besufekad *et al*., 2020). To the best of our knowledge, there is no scientific report in the literature concerning the antioxidant and antimicrobial effects of the plant.

Calotropis procera is a soft-wooded, evergreen, perennial shrub in the family Asclepiadaceae. They are commonly known as milkweeds because of the latex they produce. It includes 320 genera and 2,000 species. It is widely distributed in Asia, Africa, and America (Ramos *et al*., 2006). In Ethiopia, this plant species is known by local names of Tobiaw (Amharic), Qimbo (Afan Oromo), Ghinde'a (Tigregna), Galaqto (Afar) (Harini and Nithyalakshmi, 2017). Traditionally, *Calotropis* is used alone or with other medicines to treat common diseases such as fever, rheumatism, cold, eczema, diarrhea, and treatment of boils (Pathyusha, 2012; Abhishek *et al*., 2010). In traditional folk medicine, the plant has been employed as an antifungal and antipyretic agent (Shrivastava *et al*., 2013). In Ethiopia, the latex of *C. procera* (Asclepiadaceae) (Figure 2) is among the herbal drugs used for the treatment of blackleg to treat cattle by "Zay" people (Giday & Teklehaymanot, 2013).

Figure 2. Aerial part of *C. procera* (Adama, Oromia, Picture by Getachew Tegegn on August 16, 2020).

Previous pharmacological reports disclosed that *C. procera* exhibit wide spectrum of pharmacological activity including antimicrobial, anthelmintic, anti-inflammatory, analgesic and antipyretic, anticancer, antidiabetic, antifungal, antioxidant, larvicidal activity, anticonvulsant, anti-ulcer effects, and wound healing (Hassan *et al*., 2006; Al-Snafi, 2015). In Ethiopia, pharmacological studies of ethanolic extract from the leaves and latex *C. procera* demonstrated antimicrobial activity against *S. aureus, E. coli, Bacillus cereus, Proteus mirabilis, Proteus vulgaris, Klebsiella pneumoniae, Shigella dysenteries* and *Pseudomonas aeruginosa* (Chavan, 2016). Phytochemical studies indicated that root extracts of *C. procera* contained alkaloids, flavonoids, glycosides, saponins, and terpenes (Schimmer and Mauthner, 1996). Inspired by these reports, in the present work, chemical constituents of roots extract of *C. abyssinicum* and *C. procera*, evaluation of the antibacterial and radical scavenging activities of extracts and isolated compounds along with *in silico* molecular docking, ADMET, and Toxicity analysis were presented.

2. MATERIAL and METHODS

2.1. General Procedure

The compound purity was determined by analytical TLC. Analytical TLC was run on a 0.25 mm thick layer of silica gel GF254 (Merck) on aluminum plate. Spots were detected by observation under UV light (254 and 365 nm). The vanillin spraying agents were used as detecting reagent. Column chromatography was performed using silica gel (60-200 mesh) Merck. Samples were applied on a column by adsorbing on silica gel. The solvent was removed using rotavapor under vacuum at 40^{o}C. NMR spectra were recorded using Bruker Avance 400 MHz spectrometer.

2.2. Plant Materials Collection and Identification

The roots of *C. procera* and *C. abyssinicum* were collected from Adama and Illubabor zones of the Oromia Region, Ethiopia on August 16, 2020, and November 20, 2021, respectively. Identification and authentication of the plant's specimen were done by botanist Mr. Melaku Wondaferash at the National Herbarium, Addis Ababa University, and voucher specimens were deposited (GT-002/2020 for *C. procera* and GT-003/2021 for *C. abyssinicum*). The plants were chopped into small pieces, air dried under shade at room temperature, and pulverized using a Willy electrical mill.

2.3. Extraction and Isolation

The powdered roots of *C. abyssinicum* (800 g) and *C. procera* (550 g) were extracted with CH_2Cl_2/MeOH (1:1) 3L three times for 48h in each case by shaking using a mechanical shaker

at room temperature. The filtrates were concentrated *in vacuo* on a rotary evaporator at 40 ^{o}C to obtain 16 g (2%) reddish solid and 15.2 g (2.76 %) yellowish solid crude extracts, respectively. The mark left in each case was further extracted with methanol (100%). The filtrate was concentrated using a vacuum rotary evaporator to yield 3 g (0.375 %) reddish and 10.2 g (1.85 %) yellowish crude extracts, respectively.

The dichloromethane/methanol (1:1) roots extract (14 g) of *C. abyssinicum* was adsorbed to an equal amount of silica gel and subjected to silica gel column chromatography (200 g). Elution was done with an increasing gradient of ethyl acetate in *n*-hexane followed by methanol in dichloromethane. A total of 111 fractions were collected (each 50 mL). Concentrated fractions were subjected to thin-layer chromatography to monitor the composition profile and fractions that showed similar R_f values and the same characteristic color on TLC were combined and further purified. Combined fractions were dried in glass vials and yields were determined. Fraction 14 (1% ethyl acetate in *n*-hexane) afforded compound **1** (100 mg). Fractions 27-29 (4.5 % ethyl acetate in *n*-hexane as eluent) were combined and purified by silica gel column chromatography (eluent, gradient of ethyl acetate in *n*-hexane) to give compound **2** (90 mg). Fractions 57-59 (0.5 % methanol in dichloromethane) were combined to give compound **3** (40 mg).

The crude dichloromethane/methanol (1:1) extract (10 g) of *C. procera* was adsorbed on an equal mass of silica and subjected to silica gel column chromatography (200 g). Elution was conducted with an increasing gradient of ethyl acetate in *n*-hexane followed by an increasing gradient of methanol in dichloromethane. A total of 50 fractions were collected (each 50 mL). Fractions 22-30 showed three spots on TLC (*n*-hexane/EtOAc 4/1, 800 mg) and were further purified using silica gel column chromatography with *n*-hexane to afford 54 subfractions. Subfractions 7-11 showed a single spot (*n*-hexane: EtOAc,4:1) to give compound **4** (70 mg). Subfractions 20-31 showed a single spot (*n*-hexane:EtOAc, 7:3) to give compound **5** (60 mg). Fractions 31-34 gave single spot-on TLC (mobile phase *n*-hexane/EtOAc 7:3 as eluent) to give compound **6** (20 mg).

2.4. Antibacterial Activity

All samples were evaluated for their antibacterial activity against two-Gram positive bacteria (*Staphylococcus aureus* ATCC 25923, *Streptococcus pyogenes* ATCC 19615) and two Gram-negative bacteria (*Pseudomonas aeruginosa* ATCC 27853, *Escherichia coli* ATCC 25922) using the disc diffusion method. The microbial cultures were grown overnight at 37°C in nutrient broth, distilled water was used to adjust to 0.5 McFarland standard, and lawn inoculated onto Mueller Hinton agar (MHA) plates.100 µg were dissolved in each sample in 0.1 mL DMSO and adjusted to a concentration of 250 and 125 mg/mL. 6 mm diameter of sterile filter paper discs were soaked in 1 mL DMSO solution of the compounds at 250 and 500 µg/mL concentrations. Then, the saturated paper discs were placed on the center of every MHA plate. The inhibition zones were measured and compared with those produced by the reference antibiotics, Ciprofloxacin (each at 10 µg/disc). The resulting diameters of zones of inhibition produced by the plant extracts and standard antibiotics were measured using a ruler and reported in millimeters. The mean of zones of inhibition was calculated for each extract and the standard antibiotics. The results are expressed as M ± SEM of triplicate (Table 6) (Valgas *et al*., 2007; Singh and Jain, 2011). The standard drug used as a positive control was Ciprofloxacin, and DMSO was used as a negative control.

2.5. Antioxidant Activity Assay

The antioxidant activities of the plant extract and their constituents were studied using DPPH methods. The DPPH radical scavenging activities of the extracts and isolated compounds were evaluated using DPPH assay following procedure (Rivero-Perez *et al*., 2007). Serial dilutions

were carried out with the stock solutions 0.5 mg mL^{-1} of the plant extract and its constituents to obtain concentrations of 50, 25, 12.5, and 6.25 µg mL^{-1}. The solutions were prepared using methanol as solvent. 4 mL from each four diluted concentrations of the samples were mixed with 1 mL of 2,2-diphenyl-1-picryl hydrazyl (DPPH) solution that was prepared by dissolving 4 mg of DPPH in 100 mL of MeOH. The resulting solution was placed in an oven at 37°C for 30 min and subjected to a UV-Vis spectrophotometer to record absorbance at 517 nm. The percentage of DPPH inhibition is calculated according to the following formula (Proestos *et al*., 2013).

$$(\%)\ \text{inhibition} = \frac{(A_{control} - A_{sample})}{A_{control}} \times 100$$

Where A control was the absorbance of the DPPH solution and A sample was the absorbance of a tested sample. Samples were analyzed in triplicate. Ascorbic acid was used as a positive control.

2.6. *In silico* Pharmacokinetics (ADME), Drug-likeness and Toxicity Prediction

Computational technology has reduced experimental drug trials and improved the success rate; hence, it's become an important tool in drug candidate identification. The screening of bioavailability and pharmacokinetic properties like absorption, distribution, metabolism, and excretion parameters are evaluated to determine their activity within the human body. They evaluated using the Swiss ADME online web tool. The structures of isolated compounds were converted to their canonical simplified molecular-input line-entry system (SMILE), and the SMILES of all selected ligands were used as input data and submitted to SwissADME and PreADMET tool to estimate *in-silico* pharmacokinetic parameters such as the number of hydrogen donors, hydrogen acceptors, and rotatable bonds, and total polar surface area of a compound. The computer program further gave a compiled result on the lipophilicity and hydrophilicity of those molecules by integrating results obtained from various Log P and S prediction programs called ILOGP, XLOGP3, WLOGP, ESOL, and SILICOS-IT. Log P, a measure of the lipophilicity of the molecule is the logarithm of the ratio of the concentration of drug substance between two solvents in an unionized form. The drug-likeness of the isolated compounds was predicted by adopting Lipinski's Rule of 5. It denotes that the drugs and/or candidates should obey the rule of 5 parameters like hydrogen-bond donors (HBDs) < 5, hydrogen-bond acceptors (HBAs) < 10, a molecular mass < 500 Da, log P not > 5, and total polar surface area (TPSA) shouldn't be > 140 Å (Lipinski *et al*., 1997). The rule was developed to set drug-likeness ground rules for new molecular entities (NMEs) (Lipinski, 2000). The Rule of 5 predicts molecules with more than 5 H-bond donors, 10 H-bond acceptors, molecular weight of more than 500 Da, and also the calculated Log P (Log P) greater than 5 likely had poor absorption or permeation of the molecular entities. Hence, molecules will unlikely to become orally bioavailable as a drug if their properties fall outside these boundaries (Tareq & Khan, 2010). Lipinski's rule suggests an upper limit of 5 for druggable compounds. For the chemical substance, the lower the log P values the stronger the lipophilicity.

The absorption of drugs depends on water solubility, P-glycoprotein substrate (P-gp substrate), skin permeability (log Kp) levels, Gastro-Intestinal absorption (GSI), and membrane permeability. The drug distribution depends on the blood-brain barrier (BBB). Excretion depends upon the total clearance, and renal OCT2 substrate (Mahanthesh *et al*., 2020; Han *et al*., 2019). The volume of distribution and metabolism was evaluated with the help of CYP models, namely CYP1A2 inhibitor, CYP2C19 inhibitor, CYP2C9 inhibitor, and CYP3A4 inhibitor. The toxicity profile of the isolated compounds was predicted. ProTox-II server were accustomed to determine the toxicological endpoints (Hepatotoxicity, Carcinogenicity, Immunotoxicity, Mutagenicity), toxicity class and also the level of toxicity (LD50, mg/Kg) of

the isolated compounds (Banerjee *et al*., 2018; Drwal *et al*., 2014). The results were compared with ciprofloxacin used as a standard clinical drug (Table 9).

2.7. Molecular Docking Study

AutoDock Vina version 4.2 with the standard protocol was established to dock the proteins (PDB ID: 6F86, PDB ID: 1HD2 and PDB ID: 3T07) and also isolated compounds **2, 3, 4, 5** and **6** into the active site of proteins (Seeliger and Groot; Trott and Olson, 2010; Tapera *et al.*, 2022). The 2D structures of isolated compounds (**2, 3, 4, 5, 6**) were drawn using the ChemOffice tool (ChemDraw 16.0). ChemBio3D was used to minimize the energy of each molecule. The energy-minimized ligand molecules were then used as input for AutoDock Vina, so as to hold out the docking simulation (Trott and Olson, 2010). The crystal structures of receptor molecules *E. Coli* DNA gyrase B (PDB ID: 6F86), Pyruvate Kinase (PDB ID: 3T07), and human peroxiredoxin 5 (PDB ID: 1HD2) were downloaded from the protein data bank. All the ligands were individually docked into the target based on ligand-protein interactions. As per standard protocol protein preparation was done (Narramore *et al*., 2019), by removing the chosen water molecules, cofactors, and previously attached ligands. The protein was prepared by adding polar hydrogens using auto preparation of target protein file AutoDock 4.2.6 (MGL tools 1.5.6). To set the grid box for docking simulations the graphical user interface program AutoDock 4.2.6 was used. We tried several different docking pockets and poses, and at last, the grid was generated as per the best results achieved. The docking algorithm provided with AutoDock Vina v.1.2.0 was used to search for the best docked conformation between ligand and protein (Poustforoosh *et al.*, 2022). A maximum of nine conformers were considered for each ligand during the docking process. For analyzing the interactions between the target receptor and ligands by discovery studio visualizer and PyMOL, conformations with the most favorable (least) free binding energy were selected (Poustforoosh *et al.*, 2021). The ligands are represented in several colors, H-bonds and also the interacting residues are represented in stick model representation.

2.8. Statistical data analysis

Antibacterial and antioxidant data obtained by triplicate measurements were reported as mean ± standard error of the mean (SEM). GraphPad Prism version 8.0.2 for Windows was established to perform the analysis. Groups were analyzed for significant differences using a linear model of variance analysis (ANOVA) test for comparisons was performed.

3. RESULTS and DISCUSSION

3.1. Characterization of Isolated Compounds

The dichloromethane/methanol (1:1) extract of the roots of *C. abyssinicum* and *C. procera* was subjected to silica gel column chromatographic fractionation which afforded six compounds (**1-6**) of which compounds **1-3** were reported herein for the first time from *C. abyssinicum* whereas compound **2** was reported herein for the first time from the plant source. The structures of the isolated compounds were characterized by ^{1}H NMR, ^{13}C NMR, and DEPT-135 as discussed here below.

Compound **1** was obtained as a yellow oil with R_f value of 0.40 (*n*-hexane/EtOAc (9:1), as eluent. Its ^{1}H NMR spectrum (400 MHz, $CDCl_3$) showed signals at δ 2.3 (t, 2H, H-2), δ 5.4 (brs, 1H, H-7) and δ 0.9 (t, 3H, H-18) attributed to methylene protons attached to a carboxyl group, olefinic proton, and terminal methyl protons, respectively. The ^{13}C NMR (100 MHz, $CDCl_3$) spectral data with the aid of DEPT-135 revealed a total of 18 carbon signals of which two olefinic methine signals at δ 130.0, and 127.9, and fourteen methylene signals at δ 34.0, 31.9, 29.7, 29.6, 29.5, 29.4, 29.3, 29.3, 29.2, 29.1, 27.2, 25.6, 24.7 and 22.7 are clearly evident. The most downfield and upfield signals appearing at δ 179.9 and 14.1 attributed to the carboxyl

group and terminal methyl, respectively. The above spectral data are in good agreement with data reported in the literature for (*E*)-Octadec-7-enoic acid (Ibrahim *et al*., 2012).

Compound **2** (40 mg) was isolated as a yellow oil from the DCM/MeOH (1:1) with R_f value of 0.6 (*n*-hexane:EtOAc (5.5/4.5), as eluent). Its ^{1}H NMR spectral data (400 MHz, $CDCl_3$) showed a signal due to terminal methyl protons at δ 0.9 (3H, t, *J*= 6.7 Hz). The spectrum also displayed methylene signals at δ 2.3 (2H, t) and 1.6 (2H, brs) of which the former suggests methylene is connected to a carbonyl group. The proton signal at δ 3.7 (1H, *m*, H-2′) accounted for the presence of oxygenated methine proton connected to oxygen whereas as signals at δ 4.1 (dd, *J* = 12.0, 4.5 Hz, 2H, H-1′), 3.9 (m, 1H, H-3′a) and 3.7 (m, 1H, H-3′b) attributed to oxygenated methylene protons. The ^{13}C NMR spectrum with the aid of DEPT-135 spectrum showed a total of 20 well resolved carbon signals of which four olefinic carbons signals at δ 130.2, 130.0, 128.1 and 127.9, methylene carbon signals at δ 34.2, 31.9, 31.5, 29.7, 29.5, 29.3, 29.1, 27.2, 25.6, 24.9 and 22.7, oxygenated methylene signals at δ 65.1 and 63.3, and sp^3 oxygenated methine at δ 70.3 are clearly observed. Most downfield signals appearing at δ 174.4 are attributed to the ester carbonyl whereas the upfield signal at δ 14.1 suggests a terminal methyl group. The above spectral data is in good agreement with data reported for penicilloitins B, previously reported from marine endophytic *Penicillium* species, where the hydroxyl group at C-13 is dehydrated to double bond in case of compound **2** (Table 1) (Mourshid *et al*., 2016).

Table 1. Comparison of the spectral data of compound 2 and penicilloitins B ($CDCl_3$, δ in ppm).

Position	Compound **2**			Mourshid *et al*., 2016
	^{1}H NMR	^{13}C NMR	Multiplicity	^{13}C NMR
1		174.4	Carbonyl	174.3
2	2.3 (d, *J* = 7.2 Hz, 2H)	34.2	CH_2	34.1
3	1.6 (brs, 2H, H-3,4)	24.9	CH_2	24.8
4		25.6	CH_2	25.7
5	1.3 (d, *J* = 17.1 Hz, H-5,6,7,8)	29.3	CH_2	29.3
6		29.7	CH_2	29.7
7		29.5	CH_2	29.5
8		29.1	CH_2	29.0
9	2.0 (brq, *J* = 13.3, 5.0 Hz, 2H)	27.2	CH_2	27.3
10	5.4 (d, *J* = 11.6 Hz, 1H)	130.2	= CH	133.4
11		127.9	= CH	125.2
12		31.5	CH_2	35.3
13		128.1	= CH	71.5
14		130.0	= CH	36.8
15		31.9	CH_2	31.8
16		22.7	CH_2	22.0
17	0.9 (t, *J* = 5.0 Hz, 3H)	14.1	CH_3	14.0
1’	4.2 (d, *J* = 17.5 Hz, 1H), 4.1 (t, *J* = 6.1 Hz, 1H)	65.1	CH-O	65.3
2’	3.7 (m, 1H)	70.3	CH_2O-	70.2
3’	3.9 (d, *J* = 22.3 Hz, 1H), 3.86 – 3.75 (m, 1H)	63.3	CH_2O-	63.3

Compound **3** was obtained as a reddish crystal with R_f value of 0.56 (DCM: MeOH, 9.5:0.5) as eluent. The ^{1}H NMR spectrum (400 MHz, $CDCl_3$) showed the presence of an olefinic proton signal at δ 5.3 (brs, 1H, H-6, 7)**.** The compound exhibited the doublet signals at δ 4.1 (1H, d, *J* = 8.0 Hz, H-1′a), and 3.8 (1H, d, *J* = 7.8 Hz, H-1′b) due to oxygenated methylene protons. The

signal at δ 1.3 (brs, 6H) is the characteristic signal for many methylene protons in the compound which was supported by the appearance of an intense carbon signal at δ 29.7 in the ^{13}C NMR spectrum. The broad singlet signal observed at δ 2.3 is ascribed to methylene protons attached to a carbonyl group. An upfield proton signal at δ 0.9 (brs, 6H) is evident for the presence of two terminal methyl protons in the compound. The ^{13}C-NMR (400 MHz, $CHCl_3$) spectrum with the aid of DEPT-135 revealed 20 carbon signals of which fourteen methylene carbons at δ 34.4, 34.3, 31.9, 31.5, 29.7, 29.5, 29.4, 29.3, 28.6, 27.2, 25.9, 25.0, 24.8 and 22.7. The downfield signals at δ 64.4 correspond to an oxygenated methylene carbon and the most upfield carbon signal at δ 14.2, and 14.1accounts for the presence of two terminal methyl protons. The presence of two olefinic sp^2 signals at δ 129.9 and 129.8 suggest the presence of one double bond. The presence of ester carbonyl carbon was evident at δ 174.1. On the basis of the above spectral data, the structure of compound **3** was found to be identical to data reported for Ethyl (E)-octadec-8-enoate (Barange *et al*., 2020) reported herein for the first time from the genus *Crinum.*

Compound **4** was obtained as a yellowish solid with R_f value of 0.51 (*n*-hexane/Ethyl acetate 4/1) as eluent. Its ^{1}H-NMR spectrum (400 MHz, $CDCl_3$) showed the presence of an olefinic proton signal at δ 5.4 (m, 1H, H-4) and 5.1 (m, 1H, H-5)**.** Oxygenated methylene protons appeared at δ 4.3-4.1 (m, 1H) and 3.8-3.5 (m, 1H). An upfield proton signal at δ 0.9 (m, 3H) is evident for the presence of methyl group in the compound.

The ^{13}C-NMR spectrum with aid of DEPT-135 showed a total of well resolved 14 carbon signals including seven methylene signals at δ 33.8, 31.9, 30.4, 29.7, 29.4, 28.9, 23.7, and 22.7, methine carbon at δ 38.7, oxygenated methylene carbons at δ 63.1 and 68.2 and terminal methyl at δ 14.1, and two sp^2 methines at δ 130.9 and 128.8. The above spectral data is comparable with literature reported data for (4*Z*)-dodec-4-en-1-ol (D´yakonov *et al*., 2020) and the only difference is additional hydroxyethyl at C-2 in the case of compound **4** Table 2.

Table 2. ^{13}C-NMR spectral data of compound **4** and the reported ^{13}C-NMR data for (4*Z*)-dodec-4-en-1-ol (D´yakonov *et al*., 2020).

Position	NMR data of compound **4**			D´yakonov *et al*., 2020	
	^{1}H-NMR	^{13}C-NMR	Multiplicity	^{13}C-NMR	Multiplicity
1		63.1	CH_2O-	61.9	CH_2O-
2		38.7	CH	32.5	CH_2
3		33.8	CH_2	23.5	CH_2
4	5.38(m,1H)	128.8	= CH	128.8	= CH
5	5.1(m, 1H)	130.0	= CH	130.4	= CH
6		23.7	CH_2	27.1	CH_2
7		31.9	CH_2	31.8	CH_2
8		28.9	CH_2	29.2	CH_2
9		29.4	CH_2	29.2	CH_2
10		29.7	CH_2	29.7	CH_2
11		22.7	CH_2	22.6	CH_2
12	0.9 (m, 3H)	14.1	CH_3	13.9	CH_3
1'		30.4	CH_2	-	-
2'		68.2	CH_2O-	-	-

Compound **5** was obtained as a white solid with an R_f value of 0.46 (*n-hexane*/EtOAc (3.5:1.5) as eluent. Its ^{1}H-NMR spectrum (400 MHz, $CDCl_3$, Table 3) showed three olefinic protons at δ 5.8 (dd, 1H), 5.4 (m, 1H), 5.2 (dd, *J* = 15.1, 8.6 Hz, 1H). The signal at δ 4.4 (1H, s, H-3) corresponds to oxygenated methylene proton. The appearance of the singlets at δ 1.4, 0.8, and 0.8 confirm the presence of three methyl groups attached to quaternary carbons. The presence of the peak at δ 2.4 revealed that the methyl proton is attached to the carbonyl group.

The spectrum also revealed the presence of methyl proton signals at δ 1.0 (dd, *J* = 11.5, 7.4 Hz, 3H), 0.9 (dd, *J* = 7.1, 2.7 Hz, 3H), 0.9 (dd, *J* = 13.5, 7.4, 1.9 Hz, 9H) and 0.8 (d, *J* = 7.1 Hz, 3H).

The ^{13}C NMR ($CDCl_3$ 400 MHz, Table 3) spectrum in combination with DEPT-135 displayed 31 carbon signals corresponding to seven methyl groups at δ 20.2, 19.8, 19.5, 19.0, 14.1, 12.2, and 12.0, nine methylene groups at δ 39.6, 38.6, 37.1, 34.2, 29.7, 28.2, 24.1, 22.7 and 21.0. Eight sp^3 methine carbons were observed at δ 56.0, 55.9, 53.6, 51.2, 45.8, 40.5, 36.,1 and 31.9. The peaks observed at δ 38.0 and 42.5 in the ^{13}C NMR spectrum were absent in DEPT-135 spectrum suggesting the presence of two sp^3 quaternary carbon atoms that belong to C-10 and C-13, respectively. The spectrum also showed sp^3 oxygenated methine at δ 73.1 (C-3) and ester carbonyl at δ 168.8 along with olefinic methines at δ 126.2 (C-7), 138.1 (C-23), and 129.4 (C-22). The above spectral data of compound **5** is comparable with data reported for the spinasterol skeleton and the only difference is the presence of extra acyl moiety at C-3, in the case of compound **5**.

Table 3. ^{1}H NMR and ^{13}C NMR data of compound **5** and literature ^{13}C-NMR data of spinasterol.

Position	Compound **5**			Meneses-Sagrero, *et al*., 2017)	Yang *et al*., 2017
	^{1}H-NMR	^{13}C-NMR	Multiplicity	^{13}C-NMR	^{13}C-NMR
1		37.1	CH_2	37.2	37.2
2		31.9	CH_2	31.5	31.5
3		73.2	CH-O	71.1	71.1
4		38.6	CH_2	38.0	38.0
5		45.8	CH	40.3	40.8
6		29.7	CH_2	29.7	29.7
7	5.8 (t, 1H)	126.2	= CH	117.5	117.5
8		-	CH	139.6	139.6
9		53.6	CH	49.5	49.5
10	-	38.0	C	34.2	34.2
11		21.0	CH_2	21.6	21.6
12		39.6	CH_2	39.5	39.5
13	-	42.5	C	43.3	43.3
14		55.9	CH	55.1	55.1
15		23.1	CH_2	23.1	23.0
16		28.2	CH_2	28.5	28.5
17		56.0	CH	55.9	55.9
18		12.2	CH_3	12.0	12.2
19		12.2	CH_3	13.0	13.0
20		40.5	CH	40.8	40.3
21		19.5	CH_3	21.4	19.0
22	5.4 (1H, m)	138.1	CH	138.2	138.2
23	5.2 (1H, m)	129.5	CH	129.5	129.5
24		51.2	CH	51.3	51.3
25		31.9	CH	31.9	31.9
26		21.2	CH_3	21.1	21.4
27		21.1	CH_3	18.99	21.0
28		25.4	CH_2	25.4	25.4
29		12.0	CH_3	12.0	12.1
30	-	168.8	Ester	-	-
31		21.0	CH_3	-	-

Compound **6** was isolated as a colorless powder with an R_f value of 0.6 (*n*-hexane: EtOAc, 1:1) as eluent from DCM:MeOH (1:1) extract of the roots of *C. procera*. Its ^{1}H NMR spectrum showed two downfield protons at δ 5.4 (m, 1H, H-6) and 5.1 (t, *J* = 3.5 Hz, 1H, H-12) allocated to H-6 and H-12 and pair of doublets at δ 4.6 and 4.5 (*J* = 4.6, 2.2 Hz*)* associated with the C-30 exocyclic methylene group. A doublet proton at δ 2.2 was attributed to methine proton H-18 proton. The ^{1}H NMR spectrum also showed signals for ten methyl groups, of these, six of them were positioned at quaternary carbons corresponding to the singlet signals. The ^{13}C NMR spectrum showed carbon signals corresponding to those of the ursane-type triterpenes (Ali et al., 1998, 2000). Olefinic carbons appeared at δ 145.2 (C-5), 121.6 (C-6), 124.3 (C-12), and 139.6 (C-13), of which the former is sp^2 quaternary carbon, whereas signals of exocyclic methylene appeared at δ 154.6 (C-20) and 107.2 (C-30). The signals at δ 80.9 is attributed to sp^3 oxygenated methine at C-3. The NMR spectral data of compound **6** is in good agreement with data reported for calotroproceryl acetate A, previously reported from the same species (Table 4) (Ibrahim *et al*., 2012).

Table 4. Comparison of the ^{13}C-NMR spectral data of compound **6** and calotroproceryl acetate A ($CDCl_3$, δ in ppm).

Position	NMR data of compound 7		Ibrahim *et al*., 2012
	^{1}H-NMR	^{13}C-NMR	^{13}C-NMR
1		38.4	38.5
2		28.1	28.1
3	3.7 (1H, brs)	80.9	81.0
4		36.8	37.8
5		145.2	145.2
6	5.4 (t, *J* = 14.5 Hz, 1H)	121.6	121.6
7		32.87	33.3
8		40.0	40.0
9		48.6	47.6
10		37.7	37.7
11		23.4	23.6
12	5.14 (t, *J* = 3.5 Hz, 1H)	124.3	124.3
13		139.6	139.6
14		40.9	42.1
15		26.6	26.9
16		23.6	23.7
17		34.5	34.7
18		50.4	48.6
19		39.7	41.5
20		154.6	154.7
21		32.9	32.9
22		38.9	39.7
23		28.8	29.1
24		15.9	15.8
25		16.8	16.8
26		16.9	16.9
27		25.8	26.6
28		17.5	17.5
29		19.5	18.3
30	4.62 (dd, *J* = 4.6, 2.2 Hz, 2H)	107.2	107.1
1′	-	171.0	171.1
2′		21.3	21.3

Figure 3. Compounds isolated from the roots of *C. abyssinicum* and *C. procera*.

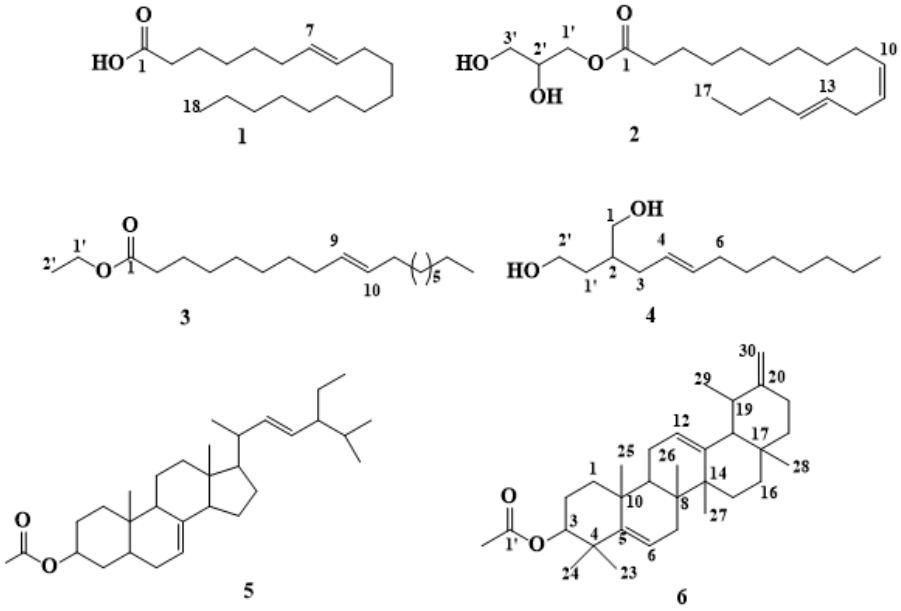

3.2. Antibacterial Activity of The Extracts and Isolated Compounds

The DCM/MeOH (1:1) root extracts of *C. abyssinicum* (Table 5, Figure 4) showed antibacterial activity against Gram-negative bacteria *P. aeruginosa* with an inhibition zone of 12.67 ± 1.76 at a concentration of 250 µg/mL and Gram-positive bacteria *S. aureus, S. pyogenes* with 16.67 ± 1.20 and 12.67 ± 1.20 mm diameter zone of inhibition at 250 µg/mL, respectively. However, unlike the above tested bacterial strains, the activity shown against *S. aureus* at 250 µg/mL was promising compared to ciprofloxacin used as a standard antibiotic. Whereas the DCM/MeOH (1:1) extract showed no activity against *E. coli*. The MeOH extracts of the root of *C. abyssinicum* (Table 5) showed activity only against Gram-negative bacteria *P. aeruginosa*, *E. coli* with a mean inhibition zone of 16.33 ± 0.33 and 10.33 ± 0.33 mm diameter at 250 µg/mL, respectively. However, the activity demonstrated against *P. aeruginosa* compared to ciprofloxacin was pronounceable.

The DCM/MeOH (1:1) extract of *C. abyssinicum* displayed better activity than the MeOH extract against *S. aureus* and *S. pyogenes*. In contrast, MeOH extract inhibited better activity against *E. coli* than DCM/MeOH (1:1) extract. Accordingly, the standard drug ciprofloxacin revealed higher antibacterial activity in comparison with the plant crude extracts. The negative control DMSO did not show any inhibition effect against the tested bacterial species. The activity showed by DCM/MeOH extract of roots of *C. procera* (Table 5, Figure 4) exhibited relatively better activity against Gram-negative bacteria with mean inhibition zone 11.67 ± 0.33 and 11.33 ± 0.67 in mm observed at 250 µg/ mL for *P. aeruginosa* and *E. coli*., respectively. Whereas *S. pyogenes* was found to inhibit moderate activity with mean inhibition zones of 10.33 ± 0.33 and 10.67 ± 0.67 mm at 125 and 250 *µ*g/mL, respectively. The MeOH extract (Table 5) showed no activity against all bacterial species used in the study. The DCM/MeOH (1:1) extract displayed better activity than the MeOH extract against all the tested bacterial species. Besides, the inhibition zone of all the extracts in the present work, the activity increased with increasing concentration in a dose-dependent manner. The MeOH root extract of *C. abyssinicum* had strong activity against *P. aeruginosa* and *E. coli* comparable to the root of *C. procera*. Similarly, its CH_2Cl_2/MeOH extract was indicated to be active against *S. aureus* with inhibition diameters 16.67 ± 1.20 and 15.67 ± 0.33 mm at 250 µg/ml and 125 µg/ml, respectively.

Compounds **1**, **2**, **4,** and **5** showed promising activity against *E. coli* with a mean inhibition zone of 13.67 ± 0.67, 14.67 ± 0.33, and 17.7 ± 0.8 mm at 250 µg/mL, respectively, compared to ciprofloxacin (31.3±0.3 mm at 250 µg/mL). Compound **2** showed moderate activity against

S. aureus (13.33 ± 0.67 mm at 250 µg/mL) compared to ciprofloxacin (26.3 ± 0.3 mm at 250 µg/mL). Compounds **1** and **4** exhibited moderate activity against *P. aeruginosa* with mean inhibition zone 10 ± 1.53 mm and 12.3 ± 1.5 mm at 250 µg/mL, respectively. The negative control DMSO did not show any inhibition effect against the tested bacterial species.

Table 5. Inhibition zone (in mm) of the DCM/MeOH (1:1), methanol root extracts and isolated compounds of C. abyssinicum and Calotropis *Procera* against selected bacterial species.

Samples	Conc. µg/mL	Inhibition zone in diameter (mm)			
		P. aeruginosa	*E. coli*	*S. aureus*	*S. pyogenes*
CH_2Cl_2/MeOH extract of *C. abyssinicum*	250 µg/mL	12.7 ± 1.8	NA	16.7 ± 1.2	12.7 ± 1.2
	125 µg/mL	11.3 ± 1.4	NA	15.7 ± 0.3	10.3 ± 0.3
MeOH extract of *C. abyssinicum*	250 µg/mL	16.3± 0.3	10.3 ± 0.3	NA	NA
	125 µg/mL	15.7 ± 0.3	9.7 ± 0.3	NA	NA
CH_2Cl_2/MeOH extract of *C. procera*	250 µg/mL	11.3 ± 0.2	11.3 ± 0.5	NA	10.3 ± 0.3
	125 µg/mL	10.7 ± 0.3	10.3 ± 0.7	NA	10.7 ± 0.7
MeOH extract of *C. procera*	250 µg/mL	NA	NA	NA	NA
	125 µg/mL	NA	NA	NA	NA
Compound **1**	250 µg/mL	10 ± 1.5	13.7 ± 0.7	NA	NA
	125 µg/mL	9.7 ± 1.2	12 ± 1.5	NA	NA
Compound **2**	250 µg/mL	NA	14.7 ± 0.3	13.3 ± 0.7	NA
	125 µg/mL	NA	13 ± 0.6	10.7 ± 0.7	NA
Compound **3**	250 µg/mL	9.3 ± 0.3	NA	8.6± 1.53	NA
	125 µg/mL	7.7 ± 0.3	NA	7.3 ± 0.3	NA
Compound **4**	250 µg/mL	12.3 ± 1.5	17.7 ± 0.8	NA	NA
	125 µg/mL	11.7 ± 1.2	16 ± 0.6	NA	NA
Compound **5**	250 µg/mL	NA	17.7 ± 1.2	NA	11.3 ± 1.2
	125 µg/mL	NA	15.7 ± 0.9	NA	9.3 ± 1.2
Ciprofloxacin	250 µg/mL	29.7 ± 0.3	31.3 ± 0.3	26.3 ± 0.3	29.7 ± 0.3
	125 µg/mL	29.3 ± 0.3	29.7 ± 0.3	26.0 ± 0.3	29.3 ± 0.3
DMSO	250 µg/mL	NA	NA	NA	NA
	125 µg/mL	NA	NA	NA	NA

NA: No activity; DMSO = Dimethyl sulfoxide; Ciprofloxacin and DMSO were used as the positive and negative controls, respectively.

Figure 4. The inhibition zone of the extracts and isolated compounds in mm (mean ± SD) at 250 μg/mL.

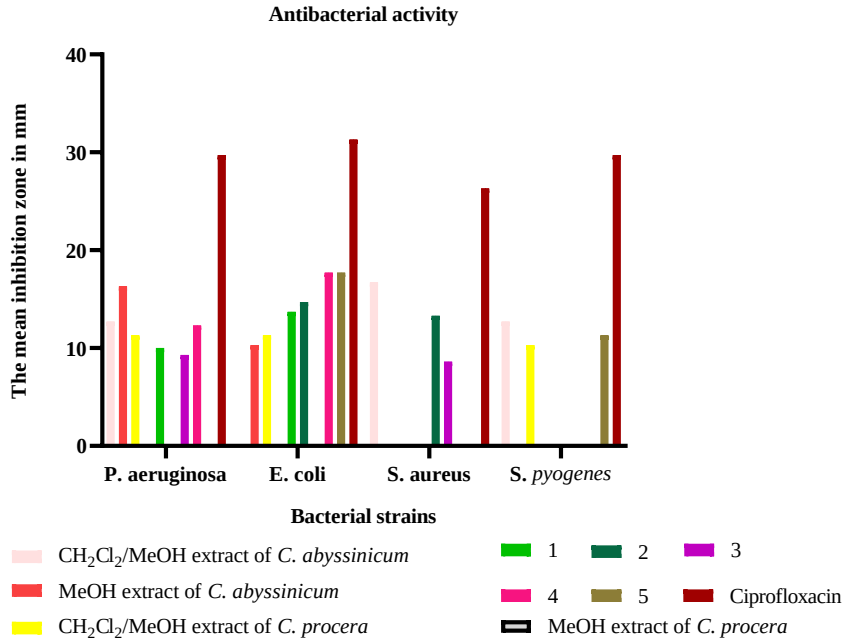

3.3. Radical Scavenging Assay

DPPH is widely used to test the ability of compounds to act as free radical scavengers and to evaluate the antioxidant activity of compounds. It is a stable free radical, which is because of the delocalized electron. The reduction capability of the DPPH radical is determined by the decrease in its absorbance at 5l7 nm (Hangun-Balkir and McKenney, 2012). The decrease in absorbance at 517 nm (Gulcin *et al*., 2010) in addition to the change in color of the DPPH from purple to yellow indicates the antioxidant activity of the samples. Furthermore, the color turns from purple to yellow as soon as the odd electron of the DPPH radical becomes paired with hydrogen from a free radical scavenging antioxidant to form the reduced DPPH-H (Luqman *et al*., 2012) (Figure 5).

Figure 5. The structure of DPPH radical and its product (DPPH-H).

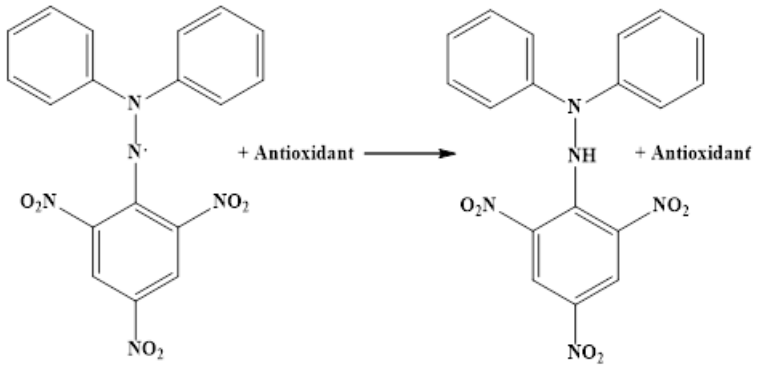

DPPH radical (Purple) DPPH-H (Yellow)

In this study, the DPPH radical scavenging activities of the *C. abyssinicum* extract and isolated compounds were examined by comparison with ascorbic acid which is used as a positive control, and the result is depicted in (Table 6, Figure 6). The results showed that the DCM:MeOH (1:1) and MeOH root extracts of *C. abyssinicum* inhibited the DPPH radical by 52.86 and 45.6 at 50 μg/mL, respectively. The result obtained was found to be moderate as compared to ascorbic acid which is used as a positive control with percent inhibition of radical by 88.10 % at the same concentration. The isolated compounds (**1-5)** from the DCM: MeOH (1:1) root extracts of *C. abyssinicum* and *C. procera* inhibited the DPPH radical by 29.53, 26.07, 62.74, 31.31, and 85.7 at 50 μg/mL, respectively. The IC_{50} values of the isolated compounds (Table 6) are calculated. The lower the IC_{50}, the higher the antioxidant activity of substances. The IC_{50} values of isolated compounds vary from 0.3 µg/mL to 20.04 µg/mL. The isolated compounds displayed lower IC_{50} values for compound **5** (85.7 %, IC_{50} value 0.30 μg/mL) which showed promising antioxidant potential as compared to ascorbic acid (88.10 %, IC_{50} value 0.14 μg/mL) used as a standard antioxidant. The activities shown by isolated compounds showed moderate antioxidant activity.

Table 6. Percent radical scavenging activity of the plants extract and isolated compounds

Tested samples	Concentration (μg/mL)				
	6.25	12.5	25	50	IC_{50}
DCM:MeOH (1:1) extract of *C. abyssinicum*	30.12 ± 0.1	36.91 ± 0.2	37.26 ± 0.1	52.86 ± 0.2	4.1
MeOH extract of *C. abyssinicum*	21.07 ± 0.4	23.69 ± 0.1	27.62 ± 0.2	45.6 ± 0.1	5.2
DCM:MeOH (1:1) extract of *C. procera*	24.29 ± 0.2	25.84 ± 0.4	27.5 ± 0.1	28.21 ± 0.1	20.0
MeOH extract of *C. Procera*	23.45 ± 0.1	26.08 ± 0.3	36.19 ± 0.2	50.48 ± 0.2	4.3
Compound **1**	18.69 ± 0.4	25.95 ± 0.2	26.07 ± 0.1	29.53 ± 0.5	10.1
Compound **2**	1.79 ± 0.1	18.45 ± 0.3	25.95 ± 0.4	26.07 ± 0.2	8.4
Compound **3**	26.55 ± 0.6	34.17 ± 0.13	39.88 ± 0.1	62.74 ± 0.12	3.3
Compound **4**	14.41 ± 0.11	19.64 ± 0.12	21.07 ± 0.11	31.31 ± 0.12	7.9
Compound **5**	52.1 ± 0.01	75.2 ± 0.04	80.9 ± 0.02	85.7 ± 0.03	0.3
Ascorbic acid	81.74 ± 0.12	85.78 ± 0.12	87.98 ± 0.12	88.10 ± 0.05	0.14

Samples were reported as Mean± SEM; Ascorbic acid was used as positive control

Figure 6. Percentage radical scavenging activities of DPPH radical by the tested samples.

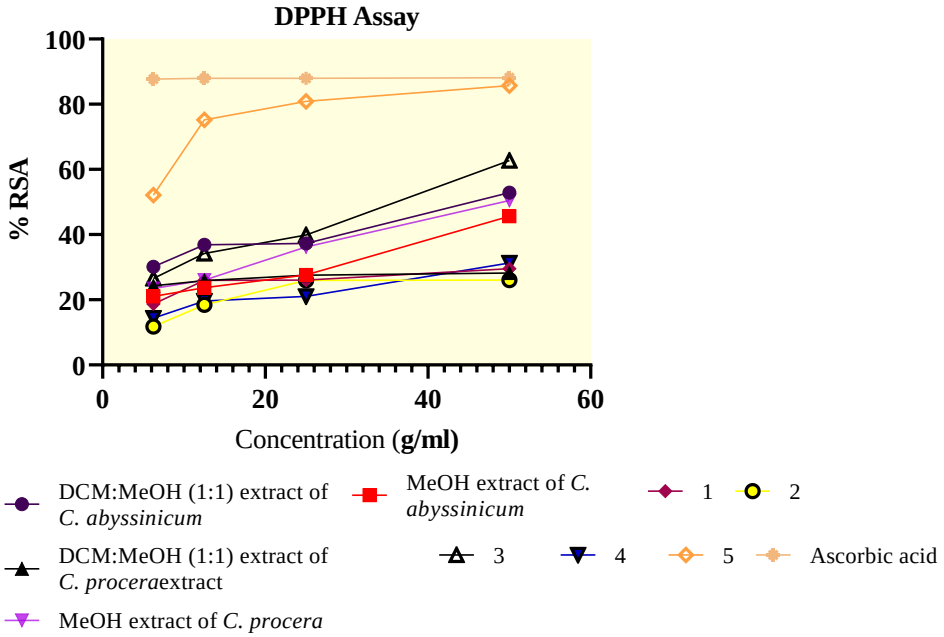

3.4. *In silico* Pharmacokinetics (ADME), Drug-Likeness and Toxicity Studies Analysis

Physicochemical properties, drug-likeness, boiled-egg model, and pharmacokinetic properties (ADME) of compounds **1-6** were determined using the SwissADME Web tool (Daina *et al*., 2017). The percent absorption (%Abs) of the was calculated using the formula %Abs=109 – 0.345 TPSA (Remko, 2009). The toxicity profile of the compounds was predicted using the ProTox-II Web tool (Banerjee *et al*., 2018). Drug-likeness is a prediction that screens whether a particular organic molecule has properties consistent with being an orally active drug (Lipinski *et al*., 1997). The drug-likeness of the isolated compounds was characterized according to "Lipinski's rule." According to Lipinski rule, the potential molecules should have the following physicochemical properties (Lipinski, 2001), such as (i) hydrogen bond donors

(HBDs) less than 5, (ii) hydrogen bond acceptors (HBAs) less than 10, (iii) a molecular mass less than 500 Da, (iv) log *P* not greater than 5, and (*v*) total polar surface area (TPSA) which should not be greater than 140 Å. In the present investigation, compounds **2, 3,** and **4** obeyed Lipinski's rule of five and are likely to be orally active. Low molecular weight (MW) signifies that the molecules are light and can easily pass through the cell membrane. Low molecular weight (MW 500) chemicals are favored for oral absorption, (Lipinski, 2001) whereas compounds with MW > 500 Da are absorbed via an alternate route, generally the membrane (Refsgaard *et al*., 2005). The present study revealed that all of the molecular weight of the studied (Table 7) compounds were less than 500 Da. An abnormal increase in values may result in a considerably lower absorption rate or poor permeation (Lipinski, C.A., 2004). The TPSA value of all the studied compounds was noticed in the range of 26.3–66.76 $Å^2$. This indicates that the results are less than 140 $Å^2$, indicating that intestinal absorption is good and if limits are beyond the score, then the drug does not possess passive cellular permeability (Turner *et al*., 2004). The optimal good bioavailability range of lipophilicity (log P) is between 0 and 3, which refers to the state of a good balance between solubility and permeability. The distribution coefficients (logP) of the isolated compounds (Table 7) were in the range of 3.36 to 5.29. The log(P) of all isolated compounds was found to be greater than three as predicted in (Table 7) which might be due to the small number of hydroxyl groups present in all compounds. Compounds that meet these criteria have been shown to have better pharmacokinetics and bioavailability characteristics. The % Abs analysis of the isolated compounds and control (Table 7) showed that all the isolated compounds have the highest percent absorption than the control.

Table 7. Drug-likeness predictions of compounds **1-6**, computed by SwissADME.

Formula	MW	NRBs	NHBAs	NHBDs	MR	TPSA	%Absn	iLOGP	Lipinski rule of five
$C_{18}H_{34}O_2$	282.46	15	2	1	89.94	37.3	96.13	4.22	1
$C_{20}H_{36}O_4$	340.5	17	4	2	100.91	66.76	85.97	4.66	0
$C_{16}H_{30}O_2$	310..51	17	2	0	99.06	26.3	99.93	5.03	1
$C_{14}H_{28}O_2$	228.37	11	2	2	71.26	40.46	95.04	3.36	0
$C_{31}H_{50}O_2$	454.73	7	2	0	142.49	26.3	99.93	5.29	1
$C_{32}H_{48}O_2$	464.72	2	2	0	143.93	26.3	99.93	4.79	1
Ciprofloxacin	331.34	3	5	2	95.25	74.57	83.27	2.24	0

NRB = number of rotatable bonds, NHD = number of hydrogen donors, NHA = number of hydrogen acceptors, and TPSA = total polar surface area.

The ability of molecules to penetrate the outer layer of the skin is described by skin permeability (Kp). The developed compounds' log Kp values (Table 8) were all determined to be within the permissible range of - 8.0 to - 1.0 (Gaur, 2015). The SwissADME prediction parameters have shown that the GIA exhibits good oral absorption except for compounds **5** and **6**. The results of the BBB permeability test performed on studied compounds (Table 8) demonstrated that compounds **1, 5,** and **6** lack BBB permeability. The P-gp affects the absorption, distribution, and clearance of a variety of substances. As a result, identifying permeability glycoprotein substrates is critical for identifying prospective medicines and optimizing them. The results show that except for compound **2,** and clinical drugs, no compounds were substrates of permeability glycoprotein (P-gp).

Table 8. ADME Predictions of studied compounds (**1-6**), computed by SwissADME and PreADMET.

Formula	log Kp (cm/s)	GI abn	BBB prn	Pgp substrate	CYP1A2 In	CYP2C19 In	CYP2C9 In	CYP2D6 In	CYP3A4 In
$C_{18}H_{34}O_2$	-2.6	High	No	No	Yes	No	Yes	No	No
$C_{20}H_{36}O_4$	-4.65	High	Yes	Yes	Yes	Yes	Yes	Yes	No
$C_{16}H_{30}O_2$	-3.69	High	Yes	No	Yes	No	No	No	No
$C_{14}H_{28}O_2$	-4.89	High	Yes	No	Yes	No	No	Yes	No
$C_{31}H_{50}O_2$	-2.46	Low	No	No	No	No	Yes	No	No
$C_{32}H_{48}O_2$	-3.45	Low	No	No	No	No	No	No	No
Ciprofloxacin	-9.09	High	No	Yes	No	No	No	No	No

logKp: Skin permeation, GI: Gastro-intestinal; BBB: Blood brain barrier; P-gp: Permeability glycoprotein; CYP: Cytochrome-P, In: Inhibitor, abn: absorption, prn: permission

Inhibitory drug metabolism fails when CYP enzymes are inhibited. Knowledge about the interaction of molecules with cytochromes (CYP) P450 enzymes is essential for the liver's drug metabolism. The results show that compound **1** inhibited cytochromes CYP1A2 and CYP2C9. Compounds **1**, **2**, and **5** act as an inhibitor for CYP2C19. All the screened compounds did not act as an inhibitor for CYP3A4, whereas compounds **2, 3,** and **4** inhibited CYP1A2. However, compound **6** did not act as any cytochrome inhibitor.

Figure 7. BOILED-Egg model for predicting gastrointestinal absorption and brain access.

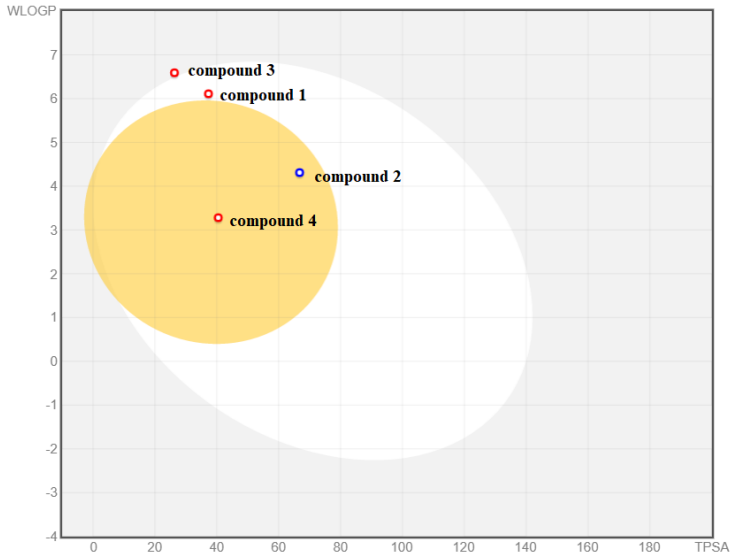

The BOILED-Egg model allowed for the correlation between the prediction of gastrointestinal (GI) absorption and blood-brain barrier (BBB) penetration with the alignment between lipophilicity (WlogP) and polarity (TPSA) properties. The white region was for a high probability of passive absorption by the gastrointestinal tract, and the yellow region (yolk) was for a high probability of brain penetration. Yolk and white areas were not mutually exclusive. In addition, the points were colored in blue if predicted was actively effluxed by P-gp (PGP+) and in red if predicted was as a non-substrate of P-gp (PGP−).

The BOILED-Egg (Figure 7) prediction model showed that compound **1** was predicted as passively absorbed but not accessing the brain (in the white) and PGP– (red dot), Whereas, compound **2** was predicted as brain-penetrant (in the yolk) and actively effluxed (blue dot). Compound **3** was predicted as not absorbed and not brain penetrant (outside the Egg). Compound **4** was predicted as brain-penetrant (in the yolk) and not subject to active efflux (red dot). Compounds **5** and **6** were predicted as not absorbed and not BBB permeant because outside of the range of the plot.

The organ toxicity (hepatotoxicity) and toxicological endpoints (carcinogenicity, immunotoxicity, mutagenicity, and cytotoxicity) of the isolated compounds and their toxicity class and LD_{50} were predicted using Pro Tox II server (Table 9). Toxicological endpoints prediction analysis indicated median lethal dose (LD50) values ranging from 48–39800 mg/Kg. Compounds **3** and **6** were predicted to be carcinogenic. Compounds **5**, and **6** were predicted to be immunotoxic. However, all the compounds including clinical drugs have shown non-hepatotoxic. Whereas compound **5** was predicted to be cytotoxic.

Table 9. Toxicity prediction of compounds **1-6**, computed by ProTox-II property explorer.

Formula	Hep	Carc	Immu	Muta	Cyto	LD50 (mg/kg)	Toxicity class
$C_{18}H_{34}O_2$	inactive	Inactive	Inactive	Inactive	inactive	48	2
$C_{20}H_{36}O_4$	inactive	Inactive	Inactive	Inactive	inactive	39800	6
$C_{16}H_{30}O_2$	inactive	Active	inactive	Inactive	inactive	5000	5
$C_{14}H_{28}O_2$	inactive	Inactive	inactive	Inactive	inactive	4300	5
$C_{31}H_{50}O_2$	inactive	inactive	active	Inactive	active	5000	5
$C_{32}H_{48}O_2$	inactive	Active	active	Inactive	inactive	3000	5
Ciprofloxacin	inactive	Inactive	inactive	Active	inactive	2000	4

Hep: Hepatotoxicity, Carc: Carcinogenicity, Immu: Immunotoxicity, Muta: Mutagenicity, Cyto: Cytotoxicity.

3.5. Molecular Docking Studies

For additional support of the *in vitro* antibacterial and antioxidant activities of the compounds, molecular docking studies of the isolated compounds (**2, 3, 4, 5,** and **6**) with the binding sites of *E. coli* DNA gyrase B (PDB ID: 6F86), Pyruvate Kinase (PDB ID: 3T07) and human peroxiredoxin 5 (PDB ID: 1HD2) were performed in order to predict the protein-ligand interactions.

In the present study, the molecular docking analysis of the isolated compounds **2, 4** and **6** was carried out to investigate their binding pattern with bacterial gyrase and the results were compared with the standard antibacterial drug ciprofloxacin (Durcik *et al.*, 2020). The result showed a binding pocket of DNA gyrase B of isolated compounds (6, **4, 2**) were found to have minimum binding energy ranging from –5.5 to –6.7 kcal/mol, respectively (Table 10). The binding affinity, H-bond, and residual interaction of compounds **2, 4,** and **6** along with ciprofloxacin are presented in Table 10. Compounds **2, 4,** and **6** showed hydrogen bond interaction with active site amino acid residue Val-120, Asn-40, and Asn-46, respectively. Compared to ciprofloxacin, compounds **2, 4,** and **6** showed significant interaction within the active site of the protein with the key amino acids Asp-73, Asn-46, Arg-76, Glu-50, Gly-77, Pro-79, Ile-78, Ile-94, Ile-78, and Ala-47. Furthermore, compounds **2, 4,** and **6** have similar residual amino acid Val-43, Val-71, Val- 167, Ile-94, Pro-79, and Ile-78 interactions and comparable binding affinities. The binding interactions of compounds **2, 4, 6,** and ciprofloxacin against *E. coli* DNA gyrase B were shown in Figure 8. The *in-silico* results are in good agreement with *in vitro* results. Hydrogen bonds between compounds and amino acids are shown as green dashed lines, hydrophobic interaction was shown as pink lines.

The molecular docking analysis of compounds **3, 5,** and **6** was carried out to investigate their binding pattern with human peroxiredoxin 5 (PDB ID: 1HD2) and compared with the Ascorbic Acid (Bernard *et al.*, 2001). The isolated compounds (**3, 5,** and **6**) were found to have minimum binding energy ranging from -2.7 to -6.5 kcal/mol (Table 11). Results obtained from the molecular docking study demonstrated that compounds **3** (-5.0 kcal/mol) and **5** (-6.5 kcal/mol) displayed higher binding affinity values compared to ascorbic acid (- 4.5 kcal/mol), while the lowest binding score was showed by compound **6** (–2.7 kcal/mol). This agrees with the

experimental findings that compounds **3** and **5** have potentially good antioxidant activity. Compared to ascorbic Acid, the isolated compounds **3** and **5** showed similar residual interactions with amino acid residues Pro-40, Thr-44, Pro-45, Arg-127, Gly-148, and Leu-149 and H-bonding interaction with Gly-46, Cys-47, and Thr-147. Compounds **3** (Arg-127, Thr-44) and compound **5** (Arg-124, Asn-76) exhibited additional hydrogen bonding interaction with amino acid residue. The binding affinity, H-bond, and residual interaction of compounds **3, 5,** and **6** are summarized in Table 11, and the binding interactions of **3, 5,** and **6** against human peroxiredoxin 5 are depicted in Figure 9.

Figure 8. The binding interactions of compounds 2, 4 and 6 against E. coli DNA gyrase B (PDB ID:6F86).

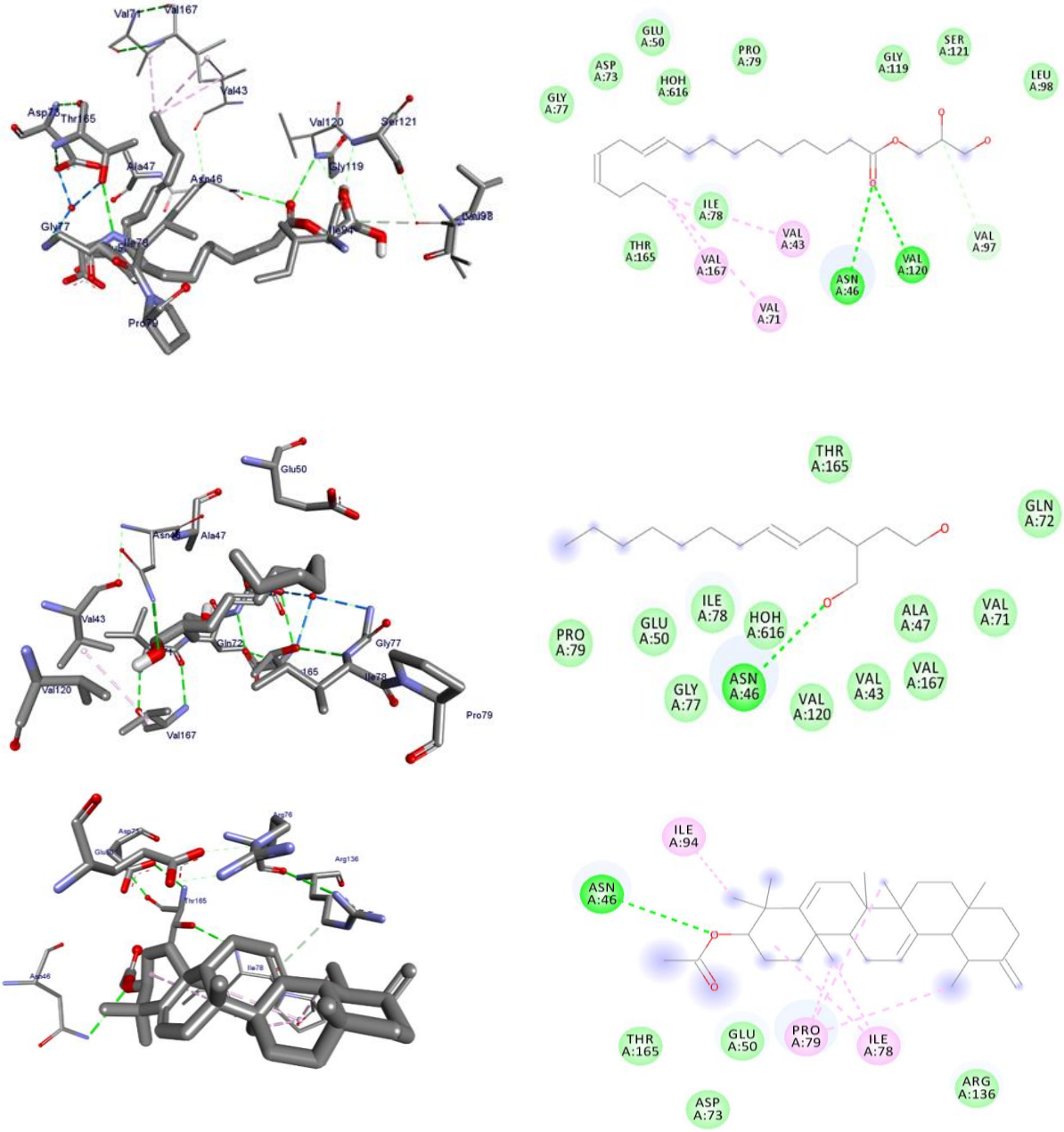

Table 10. Molecular docking scores and residual amino acid interactions of isolated compounds against E. coli DNA gyrase B (PDB ID: 6F86).

Ligands	Affinity (kcal/mol)	H-bond	Residual amino acid interactions	
			Hydrophobic/Pi-Cation	Van dar Waals
2	-6.0	Val-120, Asn-40	Val-43, Val-71, Val-167	Gly-77, Asp-73, Glu-50, Pro-79, Gly-119, Ser-121, Leu-98, Val-97, Thr-165
4	- 5.5	Asn-46	--	Val-43, glu-50, Pro-79, Gly-77, Ile-78, Thr-165, Val-120, Val-167, Val-71, Gn-72
6	-6.7	Asn-46	Ile-94, Pro-79, Ile-78	Glu-50, Asp-73, Thr-165, Arg-136
Ciprofloxacin	–7.2	Asp-73, Asn-46, Arg-76	Glu-50, Gly-77, Pro-79, Ile-78, Ile-94, Ile-78	Ala-47

Figure 9. The binding interactions of compounds **3, 5,** and **6** against human peroxiredoxin 5 (PDB ID: 1HD2).

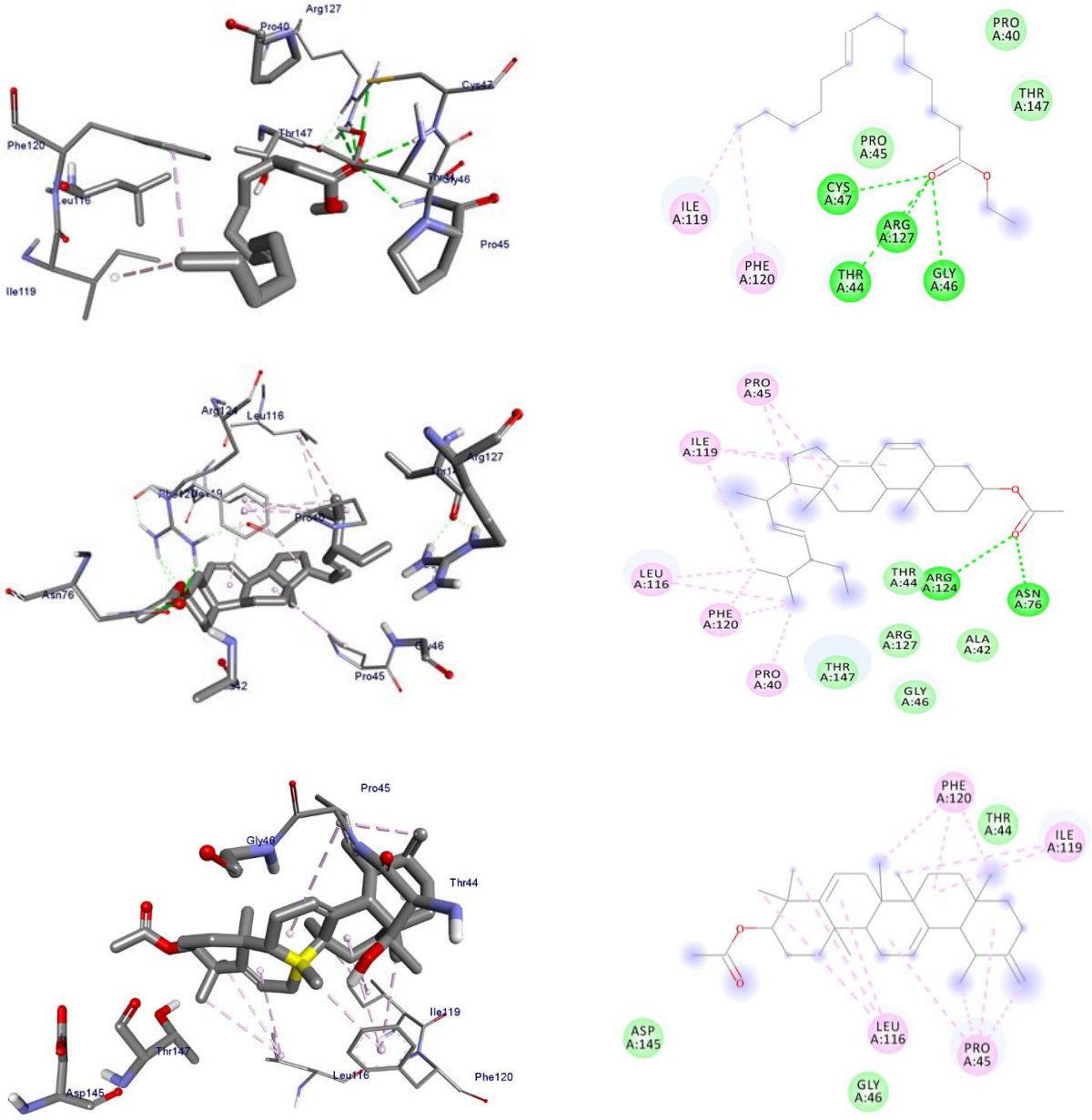

Table 11. Molecular docking scores and residual amino acid interactions of isolated compounds against human peroxiredoxin 5 (PDB ID: 1HD2).

Ligands	Affinity (kcal/mol)	H-bond	Residual interactions	
			Hydrophobic/Pi-Cation	Van dar Waals
3	-5.0	Cys-47, Arg-127, Gly-46, Thr-44	Ile-119, Phe-120	Ile-361, thr-353, Ser-354, Asn-465, Thr-464
5	-6.5	Arg-124, Asn-76	Pro-40, Pro-45, Ile-119, Phe-120, Leu-116	Ile-361, thr-353, Ser-354, Asn-465, Thr-464
6	-2.7	--	Ile-119, Phe-120, Leu-116, Pro-45	Thr-44, Asp-145, Gly-46
Ciprofloxacin	-4.5	Gly-46, Cys-47, Thr-147	---	Pro-40, Thr-44, Pro-45, Arg-127, Gly-148, Leu-149

In this study, molecular docking interactions of the isolated compound 4 and 6 against Pyruvate Kinase was studied and compared with ciprofloxacin used as an antibacterial drug (El Sayed *et al.*, 2020). The isolated compounds 4 and 6 were found to have a binding affinity of 4.5 and 5.3 kcal/mol, respectively (Table 12). Compared to ciprofloxacin, compound 4 and 6 showed similar residual interactions with amino acid residues Ile-361, Ala-358, Ser-354, Thr-353, and Thr-348 and H-bonding interaction with Ser-362 while compound 6 (Asn-465) exhibited additional hydrogen bonding interaction with amino acid residue. Binding interactions of the isolated compounds 4, 6, and ciprofloxacin against Pyruvate Kinase were shown in Figure 10.

Figure 10. The binding interactions of compounds 4 and 6 against Pyruvate Kinase (PDB ID: 3T07).

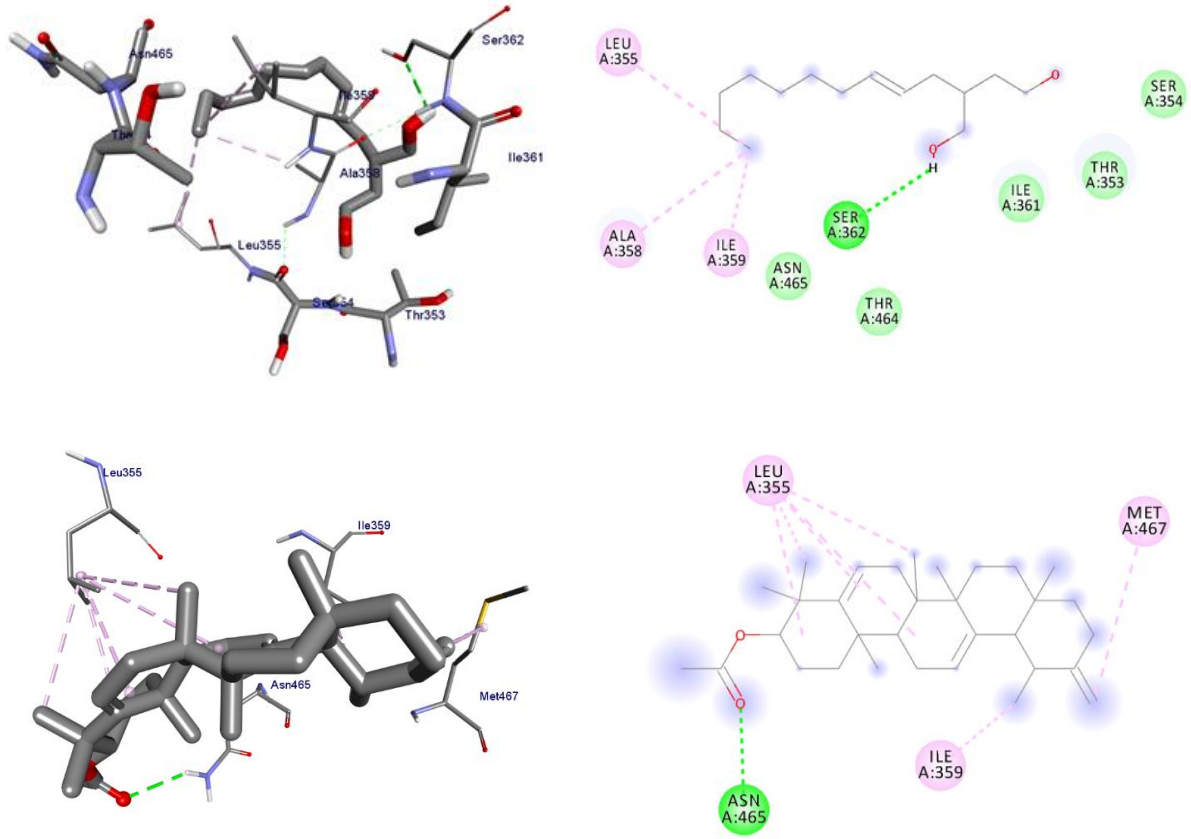

Table 12. Molecular docking scores and residual amino acid interactions of isolated compounds against Pyruvate Kinase (PDB ID: 3T07).

Ligands	Affinity (kcal/mol)	H-bond	Residual interactions	
			Hydrophobic/Pi-Cation	Van dar Waals
4	-4. 5	Ser-362	Ala-358, Ile-359, Leu-355	Ile-361, thr-353, Ser-354, Asn-465, Thr-464
6	-5.3	Asn-465	Ile-359, Leu-355	---
Ciprofloxacin	-5.6	Ser-362	Ile-361, Ala-358	Ser-354, Thr-353, Thr-348

4. CONCLUSION

The present study identified six compounds from dichloromethane/methanol (1:1) root extracts of *Crinum abyssinicum* and *Calotropis procera* of which compounds **1**-**3** were reported for the first time from *C. abyssinicum*. Compound **2**, a derivative of Penicilloitins B, was reported herein for the first time from a plant source, previously reported from culture broth of a marine endophytic *Penicillium* species. The DCM/MeOH (1:1) and MeOH root extracts of *C. abyssinicum* showed significant inhibitory activity against *S. aureus* and *P. aeruginosa* with a mean inhibition zone of 16.67 ± 1.20 mm and 16.33 ± 0.33 mm at 250 µg/mL, respectively, compared to ciprofloxacin (29.7 ± 0.3 mm and 26.3 ± 0.3 mm, respectively, at 250 µg/mL). Compounds **4** and **5** showed 17.7 ± 0.8mm and 17.7 ±1.2 mm mean inhibition zone against *E. coli*, respectively, at 250 µg/mL compared to ciprofloxacin (31.3±0.3 mm at 250 µg/mL). Compound **2** showed moderate activity against *S. aureus* (13.33 ± 0.67 mm at 250 µg/mL) compared to ciprofloxacin (26.3 ± 0.3 mm at 250 µg/mL). The results of DPPH activity showed that the DCM: MeOH (1:1) and MeOH root extracts of *C. abyssinicum* inhibited the DPPH radical by 52.86 ± 0.24 % and 45.6 ± 0.11 % at 50 µg/mL, respectively, whereas compounds (**1**-**5**) displayed 29.53, 26.07, 62.74, 31.31 and 85.7 % of inhibition, respectively, at 50 µg/mL compared to ascorbic acid (88.10 ± 0.0 % at 50 µg/mL). The drug-likeness analysis showed that compounds **2** and **4** satisfy Lipinski's rule of five with zero violations. The LD_{50} and toxicity class values obtained by *insilico* toxicity profile analysis of the compounds suggested that none of the compounds has hepatotoxicity and mutagenicity. The docking binding affinity and *in vitro* assay results suggest that compounds **2** and **6** can be considered as a potential antibacterial against *S. aureus*. Compounds **3** and **5** can be considered promising free radical scavengers. Therefore, the *in vitro* antibacterial, radical scavenging activity along with the molecular docking analysis suggest the potential use of the extracts of *C. abyssinicum* and compounds **2, 4,** and **6** as promising antibacterial agents whereas compounds **3** and **5** can be considered as promising free radical scavenger after further works which corroborate the traditional uses of the roots of the plants.

Acknowledgments

The authors are thankful to Adama Science and Technology University (ASTU) and Salale University for providing PhD study opportunity and paid leave of absence to Getachew Tegegn.

Declaration of Conflicting Interests and Ethics

The authors declare no conflict of interest. This research study complies with research and publishing ethics. The scientific and legal responsibility for manuscripts published in IJSM belongs to the authors.

Authorship Contribution Statement

Getachew Tegegn: Conducted experimental work and wrote the original draft. **Milkyas Endale** and **Yadessa Melaku:** Supervised the experimental work and edited the manuscript. Rajalakshmanan Eswaramoorthy: conducted computational analysis and edited the manuscript.

Orcid

Getachew Tegegn https://orcid.org/0000-0001-9249-384X
Yadessa Melaku https://orcid.org/0000-0003-2599-0517
Milkyas Endale Annisa https://orcid.org/0000-0002-5301-9923
Rajalakshmanan Eswaramoorthy https://orcid.org/0000-0002-8331-2100

REFERENCES

Abebe, D., Debella, A.,Urga, K. (2003). *Medicinal Plants and Other Useful Plants of Ethiopia: Illustrated Checklist*. Addis Ababa. Ethiopian Health and Nutrition Research Institute.

Abhishek, D., Mohit, C., Ashish, G., Ameeta, A. (2010). Medicinal utility of *Calotropis Procera* (Ait.) R. Br. as used by natives of village Sanwer of Indore District, Madhya Pradesh. *IJPLS*, *1*(3), 188-190

Adesanya, S.A., Olugbade, T.A., Odebiyil, O.O., Aladesanmi, J.A. (1992). Antibacterial Alkaloids in Crinum jagus, *International Journal of Pharmacognosy*, *4*, 303-307.

Ali, A.A., Hambloch, H., Frahm, A.W. (1983). Relative configuration of the alkaloid augustamine. *Phytochemistry*, *22*(1), 283–287.

Ali, M., Gupta, J., Neguerulea, M.V., Perez-Alonso, M.J. (1998). New ursan-type triterpenic esters from the roots of Calotropis gigantea. *Pharmazie*, *53*, 718– 721.

Ali, M., Ravinder, E., Ramachandram, R. (2000). New ursane-type triterpenic esters from the stem bark of Thevetia peruviana. *Pharmazie*, *55*, 385–389.

Al-Snafi, A.E. (2015). The Constituents and Pharmacological Properties of Calotropis Procera. An Overview. *International Journal of Pharma Research & Review*, *5*, 259-275

Asnakech, S., Awas, T., Gure, A. (2019). The Qualitative and Quantitative Phytochemical Investigation of Crinum Species in Ethiopia. *International Journal of Photochemistry and Photobiology*, *3*(1), 1-9.

Banerjee, P., Eckert, A.O., Schrey, A.K., Preissner, R. (2018). ProTox-II: a webserver for the prediction of toxicity of chemicals. *Nucleic Acids Research*, *46*(1), 257-263.

Barange, S.H., Raut, S.U., Bhansali, K.J., Balinge, K.R., Patle, D.S., Pundlik Rambhau Bhagat, P.R. (2020). Biodiesel production via esterification of oleic acid catalyzed by Brønsted acid-functionalized porphyrin grafted with benzimidazolium-based ionic liquid as an efficient photocatalyst. *Biomass Conversion and Biorefinery*, (2021). https://doi.org/10.1007/s13399-020-01242-7

Bekele, B., Adane, L.,Tariku, Y., Hailu, A.(2013). Evaluation of Antileishmanial Activities of Triglycerides Isolated from Roots of *Moringa stenopetala*. *Medicinal Chemistry Research*, *22*(10), 4592-99.

Bernard, A., Clippe, A., Declercq, J. P., Evrard, C., Knoops, B., & Stricht, D.V. (2001). Crystal Structure of Human Peroxiredoxin 5, a Novel Type of Mammalian Peroxiredoxin at 1.5 A Resolution. *Journal of Molecular Biology, 311(4)*, 751-759. https://doi.org/10.1006/JMBI.2001.4853

Besufekad, A., Tadesse, S., Hymete, A., Bisrat, D. (2020). Antiproliferative Effects of Alkaloids from the Bulbs of *Crinum abyscinicum* Hochst. ExA. Rich. *Evidence-Based Complementary and Alternative Medicine*, 1-8. https://doi.org/10.1155/2020/2529730

Chavan, P.A. (2016). Evaluation of Antimicrobial activity of Various Medicinal Plants Extracts of Latur Zone against Pathogens. *International Journal of Life Sciences Scientific Research*, *2*(5), 612-618.

Daina, A., Michielin, O., Zoete, V. (2017). SwissADME: a free web tool to evaluate pharmacokinetics, drug-likeness and medicinal chemistry friendliness of small molecules. *Scientific Reports*, *7*, 42717.

Döpke, W., Sewerin, E., Trimino, Z. Juliérrez, C.Z. (1981). Isolation, structure and stereochemistry of a new alkaloid from *Crinum oliganthum*. *Z Chem*, *21*(10), 358.

Drwal, M.N., Banerjee, P., Dunkel, M., Wettig, M.R., Preissner, R. (2014). ProTox: a web server for the in-silico prediction of rodent oral toxicity. *Nucleic Acids Research, 42*(1), 53–58. https://doi.org/10.1093/nar/gku401

Durcik, M., Skok, Z., Ilas, J., Zidar, N., Zega, A., Szili, P. E., Draskovits, G., Révész, T., Kikelj, D., Nyerges, A., Pál, C., Maši˘c, L. P., & Tomaši˘c, T. (2020). Hybrid inhibitors of DNA gyrase A and B design: Synthesis and evaluation. *Pharmaceutics*, *13*(1), 6. https://doi.org/10.3390/pharmaceutics13010006

D´yakonov, V.A., Makarov, A.A., Andreev, E.N., Makarova, E.Kh., Dzhemileva, L.U., Khalilov, L.M., Dzhemilev, U.M. (2020). Catalytic cycloalumination of 1,2-dienes in the total synthesis of natural grenadamide and lyngbyoic acid. *Russian Chemical Bulletin, International Edition, 69*(2), 0386-0389.

El Sayed, M.T., Sarhan, A.E., Ahmed, E., Khattab, R.R., Elnaggar, M., El-Messery, S.M., Shaldam, M.A., & Hassan, G.S. (2020). Novel pyruvate kinase (PK) inhibitors: New target to overcome bacterial resistance. *ChemistrySelect*, *5*(11), 3445-3453. https://doi.org/10.1002/slct.202000043

Fennell, C.W., Van Staden, J. (2001). *Crinum* species in traditional and modern medicine. *Journal of Ethnopharmacology*, 78(1), 15–26.Gaur, R., Thakur, J.P., Yadav, D.K, Kapkoti, D.S., Verma, R.K., Gupta, N., Khan, F., Saikia D., Bhakuni, R.S. (2015). Synthesis, antitubercular activity, and molecular modeling studies of analogues of isoliquiritigenin and liquiritigenin, bioactive components from Glycyrrhiza glabra. *Medicinal Chemistry Research., 24*(9), 3494– 3503. https://doi.org/10.1007/s00044-015-1401-1

Ghosal, S. (1981). *Special Lecture, Sixth Indo-Soviet symposium on Chemistry of Natural Products*. NCL, Pune, India, 71–72.

Giday, M., Teklehaymanot, T. (2013). Ethnobotanical study of plants used in management of livestock health problems by Afar people of Ada'ar District, Afar Regional State, Ethiopia, *Journal of Ethnobiology and Ethnomedicine, 9(*8), 1-10. https://doi.org/10.1186/1746-4269-9-8

Gulcin, I., Huyut, Z., Elmastas, M., Aboul-Enein, H.Y. (2010) Radical scavenging and antioxidant activity of tannic acid. *Arabian Journal of Chemistry*, *3*, 43–53.

Han, Y., Zhang, J., Hu, C.Q., Zhang, X., Ma, B., Zhang, P. (2019). In silico ADME and toxicity prediction of ceftazidime and its impurities. *Frontiers in Pharmacology*, *10*, https://doi.org/10.3389/fphar.2019.00434

Hangun-Balkir, Y., McKenney, M. (2012). "Determination of Antioxidant Activities of Berries and Resveratrol." *Green Chemistry Letters and Reviews, 5*(2), 147–53.

Harini, K. and Nithyalakshmi, V. (2017). Phytochemical Analysis and Antioxidant Potential of *Cucumis Melo* Seeds.*International Journal of Life Sciences Scientific Research, 3*(1), 863-867.

Hassan, S.W., Bilbis, F.L., Ladan, M.J., Umar, R.A., Dangoggo, S.M., Saidu, Y., Abubakar, M.K., Faruk, U.Z. (2006), Evaluation of antifungal acivity and phytochemical analysis of leaves, roots and stem barks extracts of Calotropis procera (asclepiadaceae), *Pakistan Journal of Biological Sciences*, *9*(14), 2624-2629.

Highet, RJ.,. (1961). Ismine. *Journal of Organic Chemistry*, *26*(11), 4767–4768. https://doi.org/10.1021/jo01069a564

Hussein, K. Eswaramoorthy, R., Melaku, Y., Endale, M. (2021). Antibacterial andAntioxidant Activity of Isoflavans from the Roots of *Rhynchosiaferruginea*and *in Silico* Study on DNA Gyrase and Human Peroxiredoxin. *International Journal of Secondary Metabolite, 8*(4), 321-336.

Ibrahim, S.R.M, Mohamed, G.A, Shaala, L.A., Laetitia Moreno Y. Banuls, L.M.Y., Goietsenoven, G.V, Kiss, R., Youssef, D.T.A. (2012). New ursane-type triterpenes from the root bark of Calotropis procera. *Phytochemistry Letters*, *5*, 490–495.

Jäger, A.K. et al. (2004). Acetylcholinesterase inhibition of *Crinum* sp. *South African Journal of Botany*, *70*(2), 323–325.

Kloos, H., Menberu, T., Tadele, A., Chanie, T., Debebe, Y., Abebe, A., Zealiyas, K., Tadele,

Lawal, A., Dangoggo, S. (2014). Phytochemical, Proximate and Toxicity Studies of Aqueous Extract of *Crinum ornatum* (Toad's Onion). *Chemical Search Journal*, *5*, 45-50.

Kloos, H., Menberu, T., Tadele, A., Tadele, A., Chanie, T., Debebe, Y., Abebe, A., Zealiyas, K., Tadele, G., Mohammed, M., & Debella, A. (2016). Traditional medicines sold by vendors in Merkato, Addis Ababa: Aspects of their utilization, trade, and changes between 1973 and 2014. *The Ethiopian Journal of Health Development*, *28*(2).

Lipinski, C.A., Franco, L., Dominy, B.W., Feeney, P.J. (1997). Experimental and computational approaches to estimate solubility and permeability in drug discovery and development settings. *Advanced Drug Delivery Reviewers*, *23*, 3-25, https://doi.org/10.1016/S0169409X(96)00423-1

Lipinski, C.A.; Franco, L., Dominy, B., Feeney, W., Experimental P.J. (1997). Computational approaches to estimate solubility and permeability in drug discovery and development settings. *Advanced Drug Delivery Reviewers*, *23*, 3-25. https://doi.org/10.1016/S0169-409X(96)00423-1

Lipinski, C.A. (2000). Drug-like properties and the causes of poor solubility and poor permeability. *Journal of Pharmacological and Toxicological Methods*, *44*(1), 235–249. https://doi.org/10.1016/s1056-8719(00)00107-6

Lipinski, C.A. (2004) Lead- and drug-like compounds: the rule-of-five revolution. *Drug Discovery Today Technologies*, *1*(4), 337–341. https://doi.org/10.101 6/j.ddtec.2004.11.007

Lipinski, C.A., Lombardo, F., Dominy, B.W., Feeney, P.J. (2001) "Experimental and computational approaches to estimate solubility and permeability in drug discovery and development settings1," *Advanced Drug Delivery Reviews*, *46*(1-3), 3–26.

Luqman, S., Srivastava, S., Kumar, R., Maurya, A.K., Chanda, D. (2012). Experimental Assessment of *Moringa oleifera* Leaf and Fruit for Its Antistress, Antioxidant, and Scavenging Potential Using *In vitro* and *In vivo* Assays.*Evidence-Based Complementary and Alternative Medicine*, 1–12.

Machocho, A.K., Bastida, J., Codina, C., Viladomat, F., Brun R and Chahabra, S.C. (2004). Augustamine type alkaloids from *Crinum kirkii*. *Phytochemistry*, *65*(23), 3143–3149.

Mahanthesh, M.T., Ranjith, D., Yaligar, R., Jyothi, R., Narappa, G., Ravi, M.V. (2020). Swiss ADME prediction of phytochemicals present in Butea monosperma (Lam.) *Tau. Journal of Pharmacognosy and Phytochemistry.*, *9*(3), 1799-1809.

Mailafiya, M.M., Pateh, U., Hassan, H.S.,2, Sule, M.I., Yusuf, A.J., Bila, A.H. (2020). Isolation and Characterization of Stigmasterol Glycoside from the root bark of Leptadeniahastata. *FUW Trends in Science and Technology Journal*, *5*(2), 394–398.

Mekuanent, T., Zebene, A., Solomon, Z. (2016). Ethnobotanical Study of Medicinal Plants in Chilga District, Northwestern Ethiopia. *Journal of Natural Remedies*, *15*(2), 88–11.

Meneses-Sagrero, S.E., Navarro-Navarro, M., Ruiz-Bustos, E., Del-Toro-Sánchez, C.L., Jiménez-Estrada, M., Robles-Zepeda, R.E. (2017). Antiproliferative activity of spinasterol isolated of Stegnospermahalimifolium (Benth, 1844*). Saudi Pharmaceutical Journal*, *25*, 1137–1143.

Mourshid,S.A., Badr, M.J., Risinger, A.L., Susan, Mooberry, L.S., Youssef, T.A. (2016). Penicilloitins A and B, new antimicrobial fatty acid esters from a marine endophytic Penicillium species. *Zeitschrift fur Naturforschung C.*, *71*(11-12), 387–392. https://doi.org/10.1515/znc-2015-0242

Narramore, S., Stevenson, C. E. M., Maxwell, A., Lawson, D.M., Fishwick, C.W.G. (2019). New insights into the binding mode of pyridine-3-carboxamide inhibitors of *E. coli* DNA gyrase. *Bioorganic and Medicinal Chemistry*, *27*(16), 3546–3550.

Demissew, S. & Nordal, I. (2010). *Aloes and other Lilies of Ethiopia and Eritrea*. Ed, 2: 1-351. Shama Books, Addis Ababa, Ethiopia.

Pathyusha, R.J.B. (2012). Potential of local anesthetic activity of Calotropis procera latex with epinephrine and pH in guinea pig. http//www.pharmatutor.org/articles/Pharmatutor-art-1043.259-275.procera - an overview, *International Journal of Pharmacy Review and Research*, 5(3).

Poustforoosh, A., Faramarz, S., Nematollahi, M. H., Hashemipour, H., Negahdaripou, M., & Pardakhty, A. (2022) In silico SELEX screening and statistical analysis of newly designed 5mer peptide-aptamers as Bcl-xl inhibitors using the Taguchi method. *Comput Biol Med 146*, 105632. https://doi.org/10.1016/J

Poustforoosh, A., Hashemipour, H., Tüzün, B., Pardakhty, A., Mehraban, M., Nematollahi, M. H. (2021) Evaluation of potential anti-RNA-dependent RNA polymerase (RdRP) drugs against the newly emerged model of COVID-19 RdRP using computational methods. *Biophys Chem., 272*, 106564. https://doi.org/10.1016/j.bpc.2021.106564

Proestos, C.H., Lytoudi, K., Mavromelanidou, O., Zoumpoulakis, P., Sinanoglou, V. (2013). Antioxidant Capacity of Selected Plant Extracts and Their Essential Oils. *Antioxidants*, *2*(6), 11–22.

Ramadan, M.A. (1986). Phytochemical investigation of the minor alkaloids and phenolic compounds of *Crinum bulbispermum*Milne. and *Crinum augustum*Rox. cultivated in Egypt. *[Thesis for Ph.D.]. Assiut University*.

Ramos, M.V. et al. (2006). Latex constituents from Calotropis procera (R. Br.) display toxicity upon egg hatching and larvae of Aedes aegypti (Linn.). *Memorias Instituto Oswaldo Cruz, Rio de Janeiro, 101*(5), 503-510.

Ramsewak, S., Nair, G., Murugsan, S. (2001). Insecticidal fatty acids and triglycerides from Dirca palustris. *Journal of Agricultural and Food Chemistry*, *49*, 5852–5856.

Razafimbelo, J., Andriantsiferana, M., Baudouin, G., Tillequin, F. (1996). Alkaloids from *Crinum firmifolium var. hygrophilum*. *Phytochemistry*, *41*(1), 323–326.

Refaat, J., Mohamed S. Kamel, Mahmoud A., Ramadan and Ahmed A. (2012). Crinum; an endless source of bioactive principles: a review, Part II. Crinum Alkaloids: Crinine-Type Alkaloids, I*nternational journal of pharmaceutical sciences and research*, *3*(9), 3091-3100.

Refaat, J., Kamel, M.S., Ramadan, M.A., & Ali, A.A. (2013). C*rinum*; an endless source of bioactive principles: a review. Part Iv: non-alkaloidal constituents, *International Journal of Pharmaceutical Sciences and Research, 4*(3), 941-948.

Refsgaard, H.H., Jensen, B.F., Brockhoff, P.B., Padkjaer, S.B., Guldbrandt, M., Christensen M.S. (2005). In silico prediction of membrane permeability from calculated molecular parameters. *Journal of Medicinal Chemistry*, *48*(3), 805-811. https://doi.org/10.1021/jm049661n

Regassa, R. (2013). Assessment of indigenous knowledge of medicinal plant practiceand mode of service delivery in Hawassa city, southern Ethiopia. *Journal of Medicinal Plant Research*, *7*, 517-535.

Remko, M. (2009). Theoretical study of molecular structure, pKa, lipophilicity, solubility, absorption, and polar surface area of some hypoglycemic agents. *Journal of Molecular Structure, THEOCHEM, 897*(1-3), 73-82.

Ridhay, A., Noor, A., Soekamto, N.H., Harlim, J., Altena, I.V. (2012). A Stigmasterol Glycoside from the root wood of Melochiaumbellata (Houtt) Stapf var. degrabrata. *Indonesian Journal of Chemistry*, *12*(1), 100–103.

Rivero-Perez, M.D., Muniz, P., Sanjase, M.L. (2007). Antioxidant profile of red coines evaluated by total antioxidant capacity, Scavenger activity, and biomarkers of oxidative stress methodologies. *Journal of Agricultural and Food Chemistry, 55*, 5476–5483.

Schimmer, O., Mauthner, H. (1996), Polymetoxylated xanthones from the herb ofCentaurium erythraea with strong antimutagenic properties in Salmonella typhimurium. *Planta Medica, 62*(06), 561-564.

Seeliger, D., De Groot, B.L. (2010). Ligand docking and binding site analysis with PyMOL and Autodock/Vina. *Journal of Computer Aided Molecular Design*, *24*, 417–422.

Shrivastava, A., Singh, S., Singh, S. (2013). Phytochemical investigation of different plant parts of calotropis procera. *International Journal of Scientific and Research Publications*, 3(8), 1-4.

Singh, R.P., Jain, D.A. (2011). Anticandidal potential of *Crinum asiaticum* leaves extract against selected oral and vaginal *Candida* pathogens. *Asian Journal of Biochemical and Pharmaceutical Research*, *1*, 283–91.

Tamiru, F., Terfa, W., Kebede, E., Dabessa, G., Roy, R.K., Sorsa, M. (2013). Ethno-knowledge of plants used in veterinary practices in Dabo Hana District, West Ethiopia.*Journal of Medicinal Plant Research, 7*(40), 2960- 2971.

Tareq, M., Khan, H. (2010). Predictions of the ADMET properties of candidate drug molecules utilizing different QSAR/QSPR modelling approaches, *Current Drug Metabolism, 11*(4), 285–295. https://doi.org/10.2174/138920010791514306

Tapera, M., Kekeçmuhammed, H., Tüzün, B., Sarıpınar, B., Koçyiğit, U. M., Yıldırım, B., Doğa, M, & Zorlue, Y. (2022). Synthesis, carbonic anhydrase inhibitory activity, anticancer activity and molecular docking studies of new imidazolyl hydrazone derivatives. *Journal of molecular structure, 1269*(133816). https://doi.org/10.1016/j.molstruc.2022.133816

Teklehaymanot, T., Giday, M., (2007; 2013). Ethnobotanical study of medicinal plants used by people in Zegie Peninsula, Northwestern Ethiopia. *Journal of Ethnobiology and. Ethnomedicine, 3,* 3-12.

Trott. O., Olson, A.J. (2010). AutoDock Vina: improving the speed and accuracy of docking with a new scoring function, efficient optimization, and multithreading. *Journal of Computational Chemistry*, *31*(2),455–461.

Turner, J.V., Maddalena, D.J., Agatonovic-Kustrin, S. (2004). Bioavailability prediction based on molecular structure for a diverse series of drugs. *Pharmaceutical Research, 21*(1), 68-82. https://doi.org/10.1023/b:pham

Valgas, C., de Souza, S.M., Smània, E.F.A., Smânia, J. (2007). Screening methods to determine antibacterial activity of natural products. *Brazilian Journal of Microbiology*, *38*, 369–80.

Wildman, W.C. (1960). *The Alkaloids: Chemistry and Physiology*. Edited by R.H.F. Manske, Academic Press.

Yang, X., Zhou, J., Wang, T., Zhao, L., Ye, G., Shi, F., Li, Y., Tang, H., Dong, Q., Zhou, X., Xu, M., Rong, Q., Chen, H., Yang, X., Cai, Y. (2017). A Novel Method for Synthesis of α-Spinasterol and its Antibacterial Activities in Combination with Ceftiofur. *Fitoterapia*, *119*, 12-19. https://doi.org/10.1016/j.fitote.2017.03.011

Yineger, H., Kelbessa, E., Bekele, T., Molla, E. (2008). Plants used in traditional management of human ailments at Bale Mountains National Park, Southeastern Ethiopia. *Journal of Medicinal Plants Research*, *2*(6), 132-153.